SANDIA REPORT

SAND2015-6334
Unlimited Release
Printed July, 2015

SANSMIC Design Document

Paula D. Weber, David K. Rudeen

Prepared by
Sandia National Laboratories
Albuquerque, New Mexico 87185 and Livermore, California 94550

Sandia National Laboratories is a multi-program laboratory managed and operated by Sandia Corporation, a wholly owned subsidiary of Lockheed Martin Corporation, for the U.S. Department of Energy's National Nuclear Security Administration under contract DE-AC04-94AL85000.

Sandia National Laboratories

Issued by Sandia National Laboratories, operated for the United States Department of Energy by Sandia Corporation.

Available to DOE and DOE contractors from
U.S. Department of Energy
Office of Scientific and Technical Information
P.O. Box 62
Oak Ridge, TN 37831

Telephone: (865) 576-8401
Facsimile: (865) 576-5728
E-Mail: reports@adonis.osti.gov
Online ordering: http://www.osti.gov/bridge

Available to the public from
U.S. Department of Commerce
National Technical Information Service
5285 Port Royal Rd
Springfield, VA 22161

Telephone: (800) 553-6847
Facsimile: (703) 605-6900
E-Mail: orders@ntis.fedworld.gov
Online ordering: http://www.ntis.gov/help/ordermethods.asp?loc=7-4-0#online

SAND2015-6334
Unlimited Release
Printed July, 2015

SANSMIC Design Document

Paula D. Weber

Geotechnology & Engineering Department
Sandia National Laboratories
P.O. Box 5800 Albuquerque, NM 87185-0706
pdgabel@sandia.gov

David K. Rudeen
GRAM, Inc.
Albuquerque, NM 87112

Abstract

The United States Strategic Petroleum Reserve (SPR) maintains an underground storage system consisting of caverns that were leached or solution mined in four salt domes located near the Gulf of Mexico in Texas and Louisiana. The SPR comprises more than 60 active caverns containing approximately 700 million barrels of crude oil. Sandia National Laboratories (SNL) is the geotechnical advisor to the SPR. As the most pressing need at the inception of the SPR was to create and fill storage volume with oil, the decision was made to leach the caverns and fill them simultaneously (leach-fill). Therefore, A.J. Russo developed SANSMIC in the early 1980s which allows for a transient oil-brine interface (OBI) making it possible to model leach-fill and withdrawal operations. As the majority of caverns are currently filled to storage capacity, the primary uses of SANSMIC at this time are related to the effects of small and large withdrawals, expansion of existing caverns, and projecting future pillar to diameter ratios. SANSMIC was identified by SNL as a priority candidate for qualification. This report continues the quality assurance (QA) process by documenting the "as built" mathematical and numerical models that comprise this document. The program flow is outlined and the models are discussed in detail. Code features that were added

later or were not documented previously have been expounded. No changes in the code's physics have occurred since the original documentation (Russo, 1981, 1983) although recent experiments may yield improvements to the temperature and plume methods in the future.

Acknowledgments

The authors wish to thank David Hart and Thomas Eyermann for a technical review of this document.

This page intentionally left blank.

Contents

List of Figures

List of Tables

Executive Summary

The United States Strategic Petroleum Reserve (SPR) maintains an underground storage system consisting of caverns that were leached or solution mined in four salt domes located near the Gulf of Mexico in Texas and Louisiana. The SPR comprises more than 60 active caverns containing approximately 700 million barrels of crude oil.

Sandia National Laboratories (SNL) is the geotechnical advisor to the SPR. As the most pressing need at the inception of the SPR was to create and fill storage volume with oil, the decision was made to leach the caverns and fill them simultaneously (leach-fill). SALT77, a Solution Mining Reseach Institute code that was used at the time, did not have the capability to run with a transient oil-brine interface (OBI). Therefore, Russo developed SANSMIC in the early 1980s (Russo, 1981, 1983). SANSMIC allows for a transient oil-brine interface (OBI) making it possible to model leach-fill and withdrawal operations. As the majority of caverns are currently filled to storage capacity, the primary uses of SANSMIC at this time are related to the effects of small and large withdrawals, expansion of existing caverns, and projecting future pillar to diameter ratios (a simple cavern stability criteria).

SANSMIC was identified by SNL as a priority candidate for qualification because of its relevance to the ullage issue. This report continues the QA process by documenting the as built mathematical and numerical models that comprise this document. The process was precipitated by recent verification exercises documented in a letter report (Rudeen et al., 2011) that concluded the current version of SANSMIC in its default mode cannot reproduce the results of bench scale experiments for oil withdrawal, direct leaching and reverse leaching found in (Reda and Russo, 1983, 1984). Also, examination of the SANSMIC source code found logic and mathematics that did not match available documentation. More recently, an investigation into the available validation data was completed (Weber et al., 2014). The current code matches with reasonable agreement the historical validation documentation (Eyermann, 1984) and the report expands upon the available validation exercises by investigating recent withdrawal leach processes for which relevant data were previously not available.

The SANSMIC design document is intended to bring more clarity and provide greater explanation to the source code. To that end: the source code and document reference each other; the program flow is outlined (see Section 1.3); details in the historical documentation are either referenced or repeated as needed for clarity; and code features that were added later or were not documented previously have been expounded. No major modifications or changes in the code's physics have occurred since the original documentation (Russo, 1981, 1983), although recent experiments may yield improvements to the temperature effects and plume methods in the future.

Future changes to the code should be thoroughly documented within the code itself, retained in SPR records in report form, and checked against the validation data utilized in (Weber et al., 2014).

The majority of this work has been inferred from reverse engineering the source code and is the best representation from the authors' perspective.

Nomenclature

BC Boundary condition

BPD Barrels per day

EOT End of tubing (depth below bradenhead flange)

FD Finite difference

HS Hanging string (depth below bradenhead flange)

inj Injection depth

LHS Left hand side

OBI Oil-brine interface (depth below bradenhead flange)

prod Production depth

QA Quality Assurance

RHS Right hand side

RW Raw water (unsaturated brine)

SG Specific gravity

SNL Sandia National Laboratories

SPR Strategic Petroleum Reserve

This page intentionally left blank.

Chapter 1

Introduction

The United States Strategic Petroleum Reserve (SPR) maintains an underground storage system consisting of caverns that were leached or solution mined in four salt domes located near the Gulf of Mexico in Texas and Louisiana. The SPR comprises more than 60 active caverns containing approximately 700 million barrels of crude oil.

Sandia National Laboratories (SNL) has been the geotechnical advisor to the SPR since its inception. As the most pressing need at the inception of the SPR was to create and fill storage volume with oil, the decision was made to leach the caverns and fill them simultaneously (leach-fill). SALT77, a Solution Mining Reseach Institute code that was used at the time, did not have the capability to run with a transient oil-brine interface (OBI). Therefore, Russo developed SANSMIC in the early 1980s. SANSMIC allows for a transient OBI making it possible to model leach-fill and withdrawal operations. As the majority of SPR caverns are currently filled to storage capacity, the primary uses of SANSMIC at this time are related to the effects of small and large withdrawals, expansion of existing caverns, and projecting future pillar to diameter ratios.

1.1 Software QA

In a prior milestone report (Rudeen and Lord, 2011), SNL outlines a plan for qualifying and baselining the software it uses in support of the vapor pressure project at the SPR. The report provides an inventory of software in use at SNL for support at the SPR and outlines the process to qualify the software. With significant project interest in maintaining accuracy, relevance, and traceability of the software tools, Quality Assurance (QA) principles are being used by SNL as the framework for software development modification and documentation. The process consists of four basic developmental phases that specify the software's 1) requirements, 2) design, 3) verification, and 4) user instructions. *Requirements* are the specific required functionalities, capabilities or attributes of the software or software modification. The *design* describes how the requirements are implemented and programmed and includes mathematical models, numerical models, program flow and data constructs. User interaction with the software is described in a *user's guide*, and *verification* demonstrates that the software correctly implements the requirements. That is, verification demonstrates that the mathematical equations are solved correctly. A second verification step, sometimes

called validation, answers the question: Is the software valid for its intended use? Validation is performed by comparison with experimental or operational data. Ancillary to the QA process is configuration management or version control of the qualified software and documentation.

The above software QA approach is designed for the development of software from inception to implementation, but the process can be applied to existing software by mapping existing documentation to the developmental phases described above, or by reverse engineering, where the capabilities, mathematical and numerical models, and program design are backed out of the source code. Reverse engineering can be difficult and time consuming, but results in as-built documentation which is essential for proper code usage.

SANSMIC (Russo, 1981, 1983) was identified by SNL as a priority candidate for qualification because of its relevance to the ullage issue. This report continues the QA process by documenting the as built mathematical and numerical models comprising the current version of SANSMIC. The process was precipitated by recent verification exercises documented in a letter report (Rudeen et al., 2011) that concluded the current version of SANSMIC in its default mode cannot reproduce the results of bench scale experiments for oil withdrawal, direct leaching and reverse leaching (Reda and Russo, 1983, 1984). Also, examination of the SANSMIC source code found logic and mathematics that does not match available documentation. More recently, an investigation into the available validation data was completed (Weber et al., 2014). The current code matches with reasonable agreement the historical validation documentation (Eyermann, 1984) and the report expands upon the available validation exercises by investigating recent withdrawal leach processes for which relevant data were previously not available.

1.2 Leach Modes

The three types of leaching operations that are utilized at the SPR and modeled by SANSMIC are withdrawal, direct, and reverse leaching. Withdrawal leach requires only one hanging string (HS) (presumably set below the OBI depth to avoid creating a stable emulsion layer) through which raw water (RW) is injected into the cavern, displacing the oil (see Figure 1.1). Withdrawal leach results in more leaching near the injection string depth tapering up to the OBI depth. The figure below shows the configuration for an idealized single well cavern.

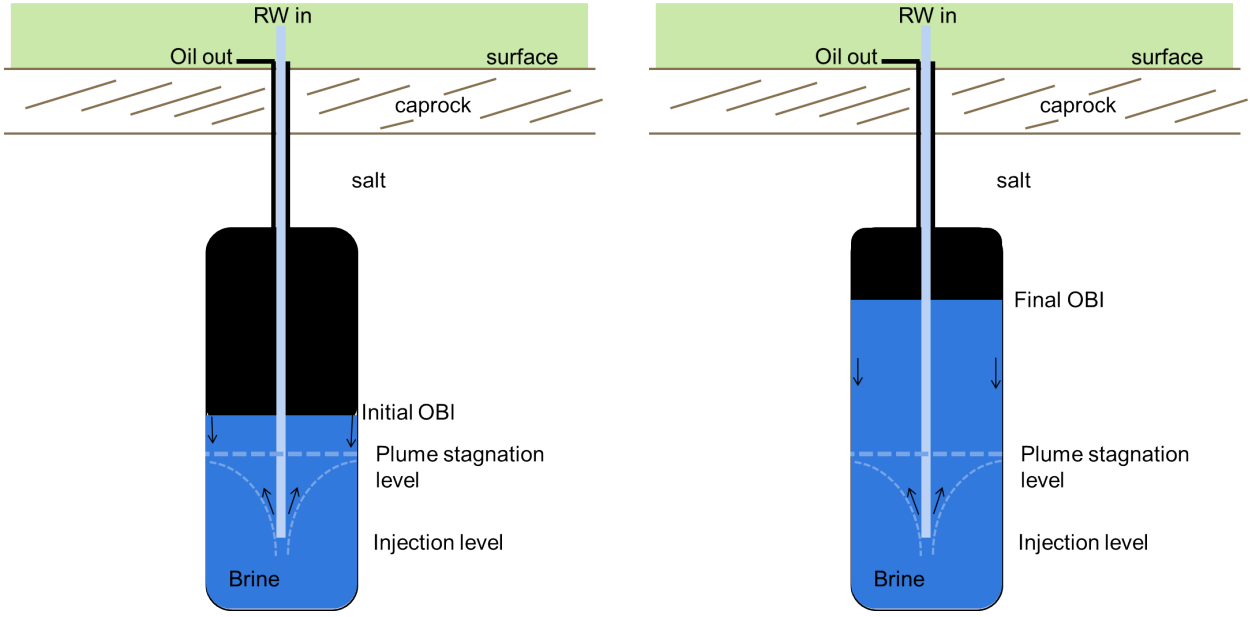

Figure 1.1: Leach configuration and flow regions for withdrawal leach with the left showing the initial leaching and the right showing the later leaching in which the OBI has moved up within the cavern.

Both direct and reverse leach configurations require two hanging strings and, if the resulting geometry is to be more precisely controlled, a controlled OBI depth as well. In direct leach, the injection depth is set below the production depth (see Figure 1.2) from which saturated or nearly saturated brine is withdrawn from the cavern. The typical leach pattern for a direct leach is increased leaching near the injection depth tapering up to the production and OBI depths. The figure below shows the configuration for a single well cavern in which the injection depth is shown in light blue, the production depth is shown in dark blue, and the oil depth is shown in black. For a single well cavern, oil and production volumes are injected or withdrawn through concentric annuli surrounding the injection string as shown. A double well cavern can result in a horizontal shift of the injection or production string depth which would induce an additional horizontal component to the brine flow within the cavern which cannot be modeled by SANSMIC. Instead, SANSMIC simulates the development of an axisymmetric cavern with injection and production locations on the axis.

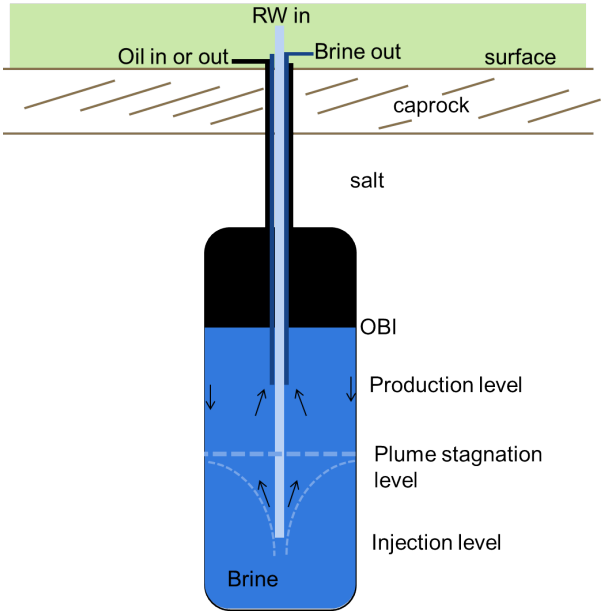

Figure 1.2: Leach configuration for direct leach.

The reverse leach sets the injection depth above the production depth (see Figure 1.3) and has a leach pattern in which the greatest amount of leach occurs from the OBI depth down to the injection depth and then tapers down to the production depth. The figure shows the configuration for an idealized single well cavern in which the injection depth is shown in light blue, the production depth is shown in dark blue, and the oil depth is shown in black. Oil movements now occur through the concentric annuli about the production string.

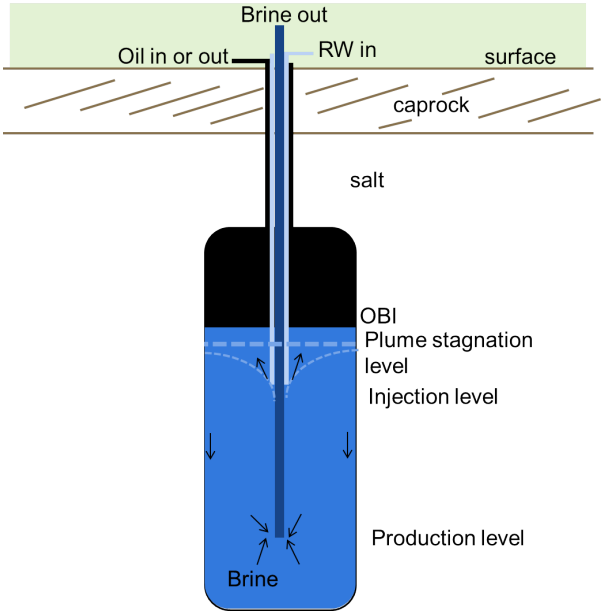

Figure 1.3: Leach configuration for reverse leach.

A summary of the three types of leaching operations modeled by SANSMIC are shown

schematically in Figure 1.4. The injection depth is shown with a solid blue line, the production depth is shown with a dashed gold line, and the OBI is shown with a horizontal black line with movements depicted with an arrow. The available data for reverse leaches used in (Weber et al., 2014) included leach-fill operations in which leaching occurs while the caverns are simultaneously being filled with oil and therefore Figure 1.4 depicts the reverse leach with a downward moving OBI. Another important characteristic of a cavern is its ullage. Ullage is the available oil storage volume remaining in the cavern i.e. the volume between the OBI depth and the end of tubing (EOT) (minus an additional $\approx$ 10 ft as a safety factor).

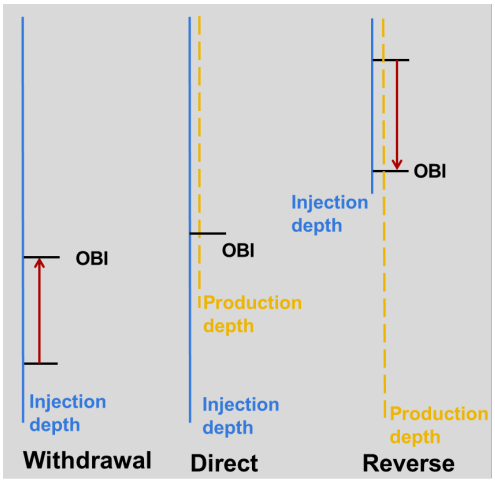

Figure 1.4: String configurations for withdrawal, direct, and reverse leach.

1.3 SANSMIC Structure

The basic components of the SANSMIC leaching model are 1.) an advective-diffusive mass balance equation (see Chapter 2), 2.) an injected raw-water plume model (see Chapter 3), and 3.) a wall recession rate model (see Chapter 4). The advective-diffusive mass balance equation includes both externally induced flow and boundary layer transport terms. The wall recession rate model is the source term for the mass balance equation. The wall recession rate model includes several adjustment factors and terms that are set depending on string positions and plume stagnation level.

A flow diagram outlining SANSMIC's calculations and processes is presented in Figure 1.5. Each section (read input, calculate injection settings, calculate plume model and dissolution rates, modify radius, finish timestep) is expanded in greater detail in Figures 1.6 - 1.10 with the remainder of the outline repeated for consistency (in the same lighter shade of green as shown here). First the input file is read, then the initial conditions for the plume model are determined, the plume stagnation level and dissolution rates are found, the change in cavern radius is calculated, and the timestep is adjusted. If the current timestep does not end the stage, the code re-updates the injection data. If the current timestep concludes the stage

but not the leach simulation, the code progresses by reading the next stage of the input file. If the current timestep concludes the stage and it is the final stage, the program finalizes output and terminates.

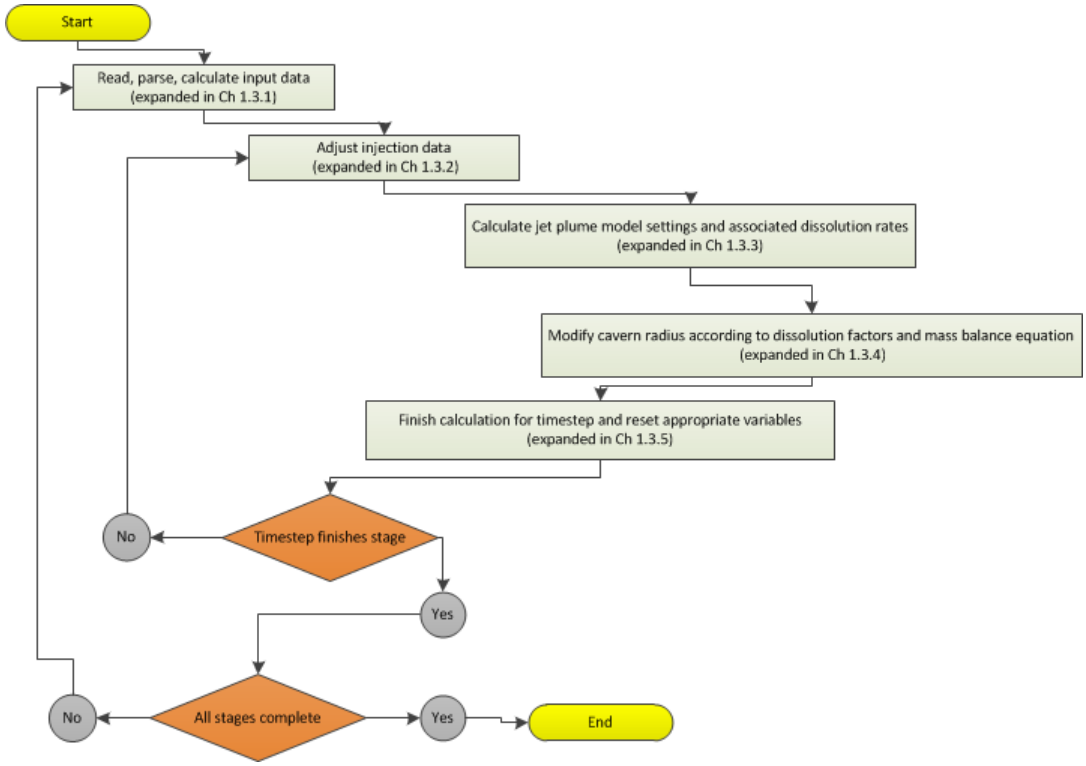

Figure 1.5: Summary flow diagram of SANSMIC.

1.3.1 Data Input

The details of the "read input data" section are given in Figure 1.6. A single stage of the input file is read, parsed, and echoed to the log file. The initial conditions for the injection plume model are determined. For the first stage, cavern geometry is then read and the geometry and associated settings are initialized. The reading of the input data for the current stage is now complete and the code continues to next process phase. Injection, production, and OBI depths are identified in the figure as inj, prod, and OBI respectively.

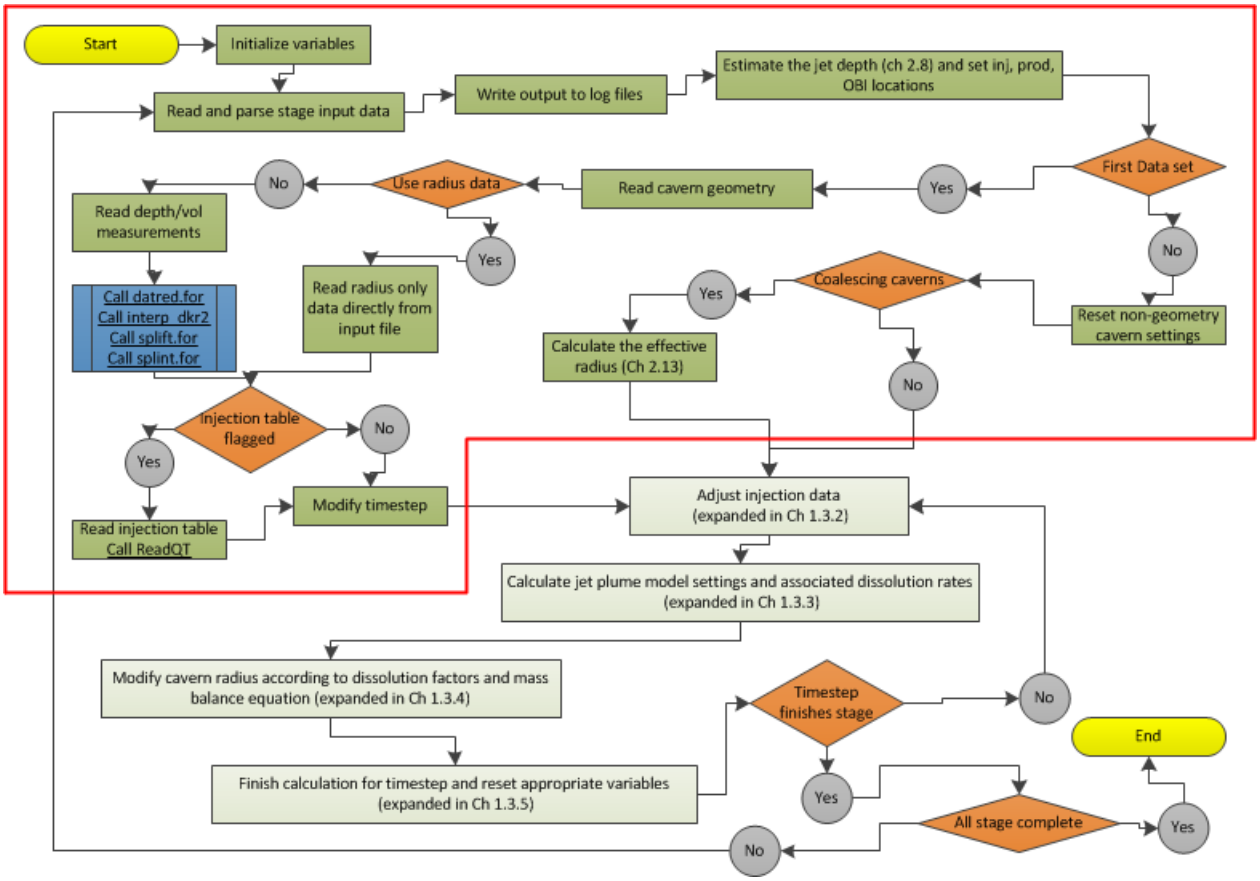

Figure 1.6: Detailed flow diagram of the input data section of SANSMIC.

1.3.2 Initial Setup and Configuration

The details of the second section (calculate injection settings) are given in Figure 1.7. If the leach type is set to withdrawal leach, the production depth is maintained at or below the OBI and timestep is modified to ensure that the OBI does not change more than one cell per timestep. The temperature correction factor for the dissolution rate is then calculated, but is not currently used. If the injection rate is different than the prior timestep, the initial conditions for the injection plume are recalculated. If the oil and RW injection rates are given in table form as opposed to a single value per stage, the value of the current timestep is determined as retrieved by the routine GetQ.for. The injection volumes are tallied for output. Injection, production, and OBI depths are identified in the figure as inj, prod, and OBI respectively and specific gravity is abbreviated to sg.

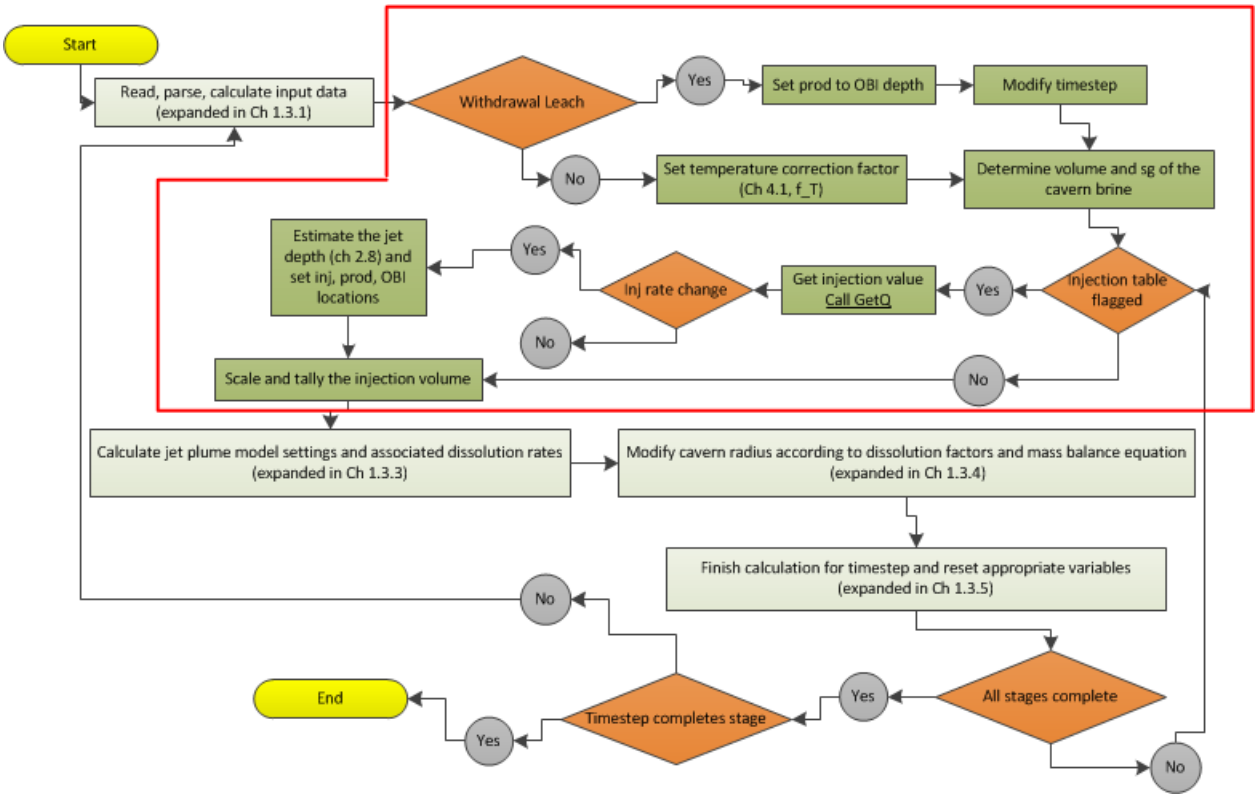

Figure 1.7: Detailed flow diagram of the injection calculations and settings of SANSMIC.

1.3.3 Plume and Dissolution Rate Models

The details of the third section "calculate plume model and dissolution rates" are given in Figure 1.8. Every third timestep the plume model is called to solve a system of three ordinary differential equations (ODEs) for volume balance, momentum balance, and density deficiency (plume.for, ode.for, de.for, step1.for, and interp.for). Next the wall recession rate is determined based on the SG of the cavern brine next to the wall and a set of salt dissolution adjustment factors are determined based upon the relative positions of the injection, production, and the plume stagnation depths. If the type of leach is leach/fill, the total injected volumes (oil and brine) and the OBI are updated which completes the plume model and dissolution rate evaluations.

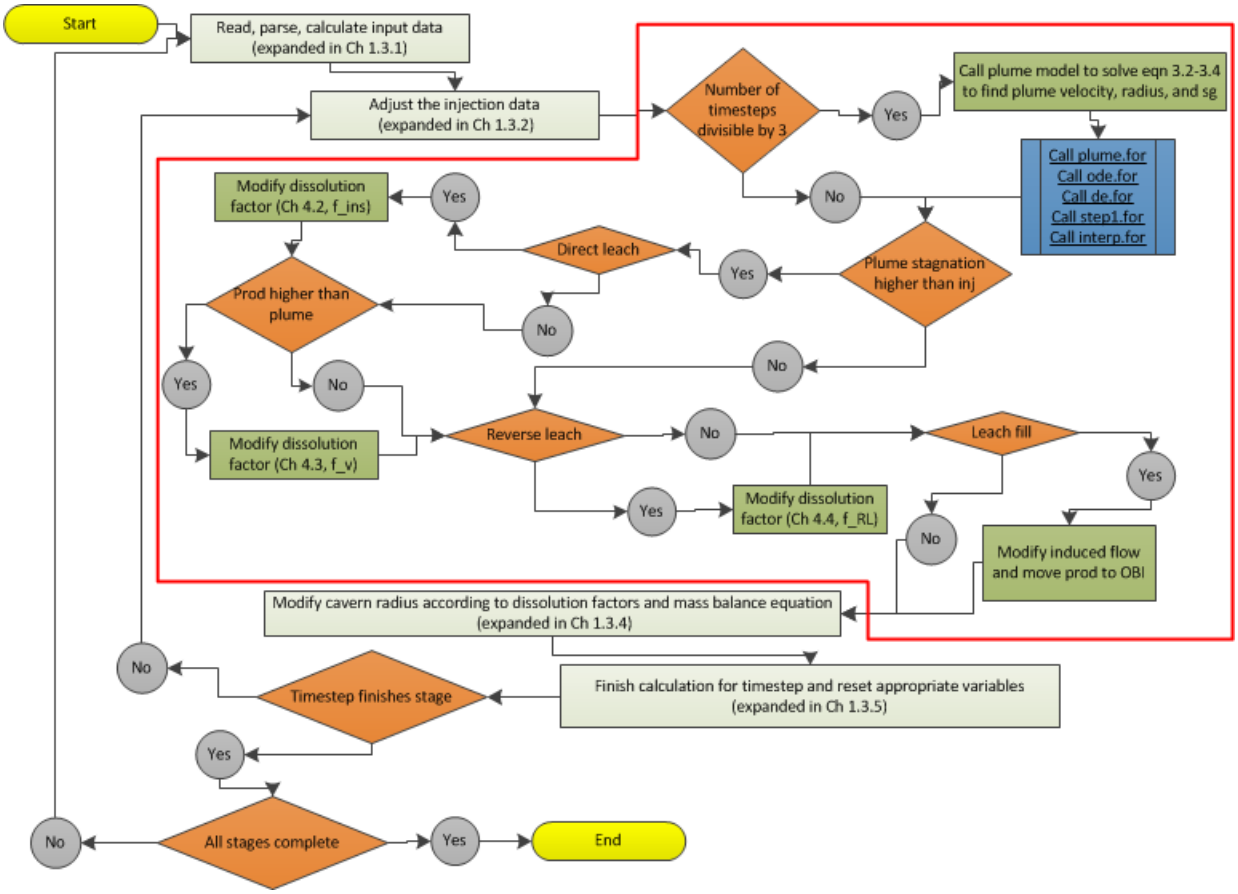

Figure 1.8: Detailed flow diagram of the plume and dissolution rate calculations of SANSMIC.

1.3.4 Adjust Cavern Radius

The details of the fourth section "modify cavern radii" are given in Figure 1.9. The wall angle correction factor is determined, the recession rate is evaluated and adjusted, the specific gravity within the plume is found (Eqn. 2.10), the recession rate is further adjusted, and the diffusion coefficient is found. The cavern radii are now modified by the routine remove.for. The increase in insolubles is accounted for and the boundary conditions (BC's) are modified. The tridiagonal matrix of equations for the mass balance equation (Eq. 2.1) are solved using the routine trigad.for and the cavern brine is further adjusted before the new brine mass is calculated completing the modification of the radius phase. The code then continues to the next and last section of finalization.

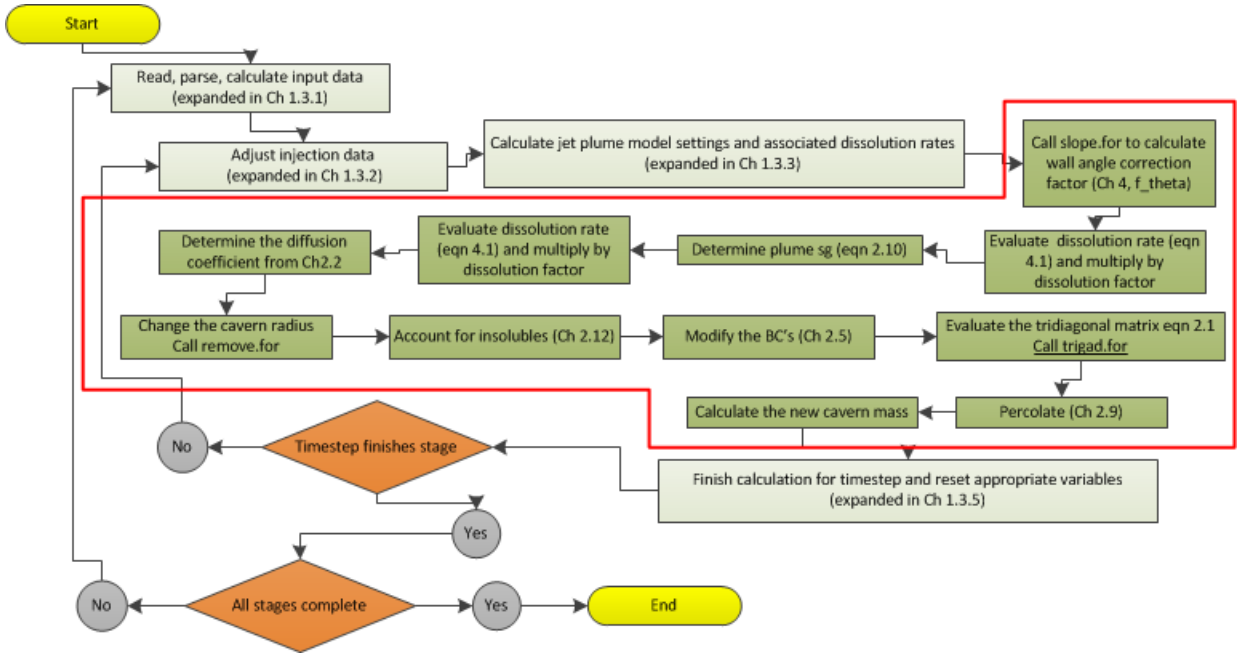

Figure 1.9: Detailed flow diagram of the cavern radius modifications and mass balance equation evaluation of SANSMIC.

1.3.5 Leach Stage Finalization and Output

The detail of the fifth and last section "finalization" is given in Figure 1.10. If the leach type is leach/fill or withdrawal, the OBI location is modified. The mass balance correction factor, new wall angle, and the ullage are determined. The output files are updated and the timestep is adjusted. If the timestep does not complete the current stage, the code returns to setup and configuration phase (Section 1.3.2). If the timestep completes the stage but another stage remains, the code returns the input phase to read new stage data (Section 1.3.1). If the timestep completes all the stages within the input file, the program performs final data output and terminates.

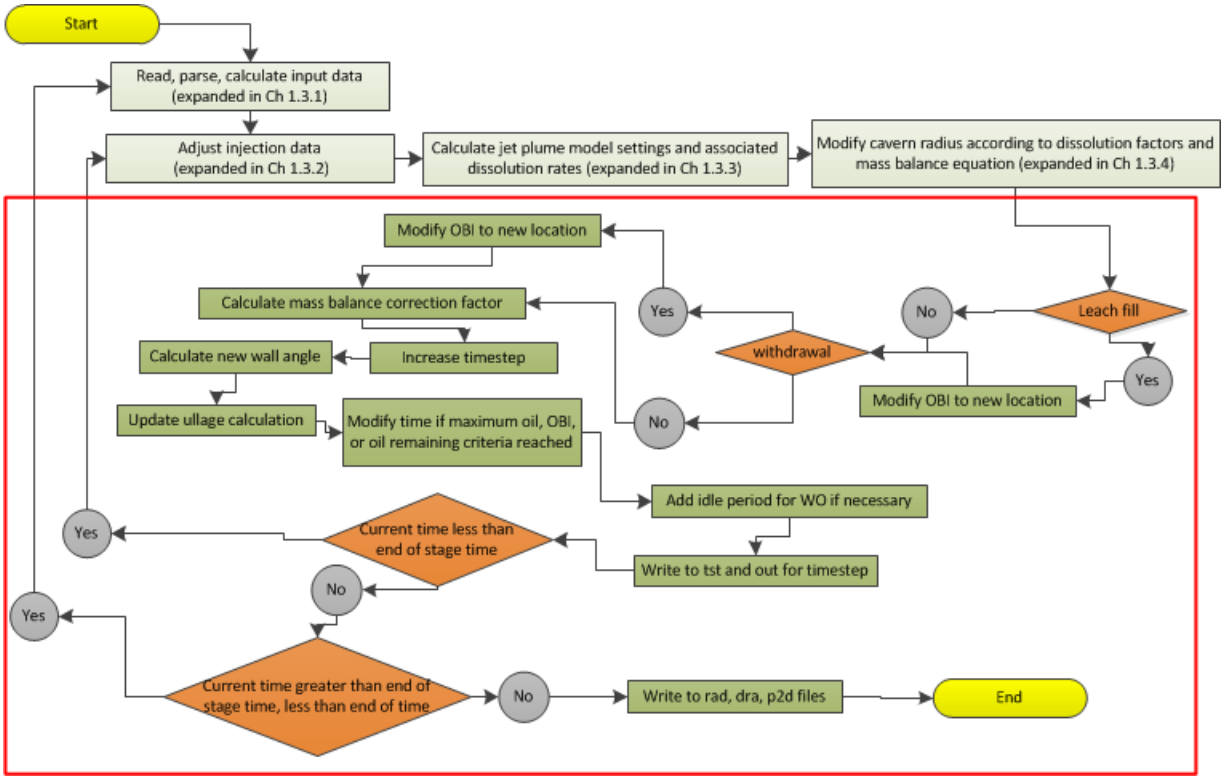

Figure 1.10: Detailed flow diagram of the timestep finalization of SANSMIC.

1.4 Report and Coding Notation

The following discussion includes a mixture of mathematical and numerical models used by SANSMIC that were either undocumented or are different than documented in (Russo, 1981, 1983). The numerical models were extracted from the source code and compared to those in Russo's original documentation and reported below as implemented in the SANSMIC code. Some discussions from (Russo, 1981, 1983) have been repeated for clarity. The notations used throughout the report are as follows: $()_+$ is used to designate that the term is to be used only if it is positive. The spatial grid is $i = 1, 2, 3, ..., M$ where 1 is the bottom and M is the top of the cavern. The time grid is $n = 1, 2, 3, ..., N$ where N is the final timestep.

Appendix B contains a sample input file and associated variable descriptions. The units utilized in the code are not standardized throughout the code and great care must be taken to use the appropriate units for each variable in the input file. The details of the input and output files (including the expected units) will be discussed in detail in the upcoming User's Manual.

An eddy diffusion coefficient is used in place of the standard free-water diffusion coefficient when the SG gradient is unstable (increasing with height). The plume model determines

the injected raw-water plume stagnation elevation (z_{plm}). This elevation along with the raw-water injection and brine production elevations (z_{inj}, z_{prd}) divide the computational grid into regions that are used to define or set model parameters.

A table of variables used in the report and the corresponding variable within the code is presented in Table 1.1. The name used throughout this report, the current name used within the code, the variable type, and any further comment or description is included. Selected variable names were updated within the code to improve readability. A list of all variable names that were changed within the code is available in the source code comments; the description of A1Main.for; and in Appendix C. Comments have been added to the source code to clarify the flow through the program. Comments corresponding to this report are referenced with the current SAND report number (SAND2015-6334). SANSMIC remains structured as it was originally written meaning that the majority of the code is in one routine reflecting the coding style of the early 1980s.

Sect.	Report name	Coding name	Type	Comment
	C	CO	vector	specific gravity
	r	cavRadius	vector	cavern radius
2.2	β	diffBeta	real	
2.2	D_{mol}	diffCoef_Mol	real	
2.2	D_0	diffD_0	real	
2.2	D	diffCoef	real	
2.3	S_d	S_d	real	wall bndry. src. coeff.
2.3	w	w		dissolution salt weight %
2.3	V_{sr}	volRemove	vector	volume of salt removed
2.3	θ	THET	vector	
2.3	A			cross-sectional area
2.6	M^{sr}	totBrineWeight	real	brine vol. * brine sg
2.6	$\overline{C}$	C_bar	real	
2.6	V_{plm}	totVolPlume	real	
3	b	plumeRad	vector	
3	u	plumeVel	vector	
4	f_θ, f_d,	DISFAC	real	*modified throughout code*
	f_T, f_{RL},	DISFAC (cont.)	real	
	f_{ins}, f_v	DISFAC (cont.)	real	

Table 1.1: List of Variables used within this report and their description.

Chapter 2

Mass Conservation Equation

The basic equation solved by SANSMIC is the following mass balance equation in axi-symmetric geometry ((Rahm and Walin, 1979a,b; Walin, 1971)) and also found as Equation 2 of (Russo, 1981) and Equation 3 of (Russo, 1983).

$$\frac{\partial C}{\partial t} + \left(\frac{M_0}{A} - \frac{2D}{r}\frac{\partial r}{\partial z}\right)\frac{\partial C}{\partial z} + \frac{2DS_d}{r\cos\theta}\left(C - \hat{C}\right) = D\frac{\partial^2 C}{\partial z^2} \tag{2.1}$$

where:

C = specific gravity

t = time

M_0 = total externally induced volume flow rate (due to raw water injection

A = cavern cross-sectional area

D = diffusion coefficient of salt in water

r = cavern radius

z = vertical elevation from cavern bottom

S_d = source coefficient defining the wall boundary condition by:

$\left.\frac{\partial C}{\partial \xi}\right|_{\xi=0} = S_d(C - \hat{C})$; where ξ is the distance from the wall

θ = wall angle with respect to the vertical

$\hat{C}$ = specific gravity of the brine at the wall (set to saturated value 1.202)

The more traditional transport equation form is given as:

$$\frac{\partial C}{\partial t} + u\frac{\partial C}{\partial z} + \gamma(C - \hat{C}) = D\frac{\partial^2 C}{\partial z^2} \tag{2.2}$$

where:

$$u = \left(\frac{M_0}{A} - \frac{2D}{r}\frac{\partial r}{\partial z}\right) : \text{net fluid velocity}$$

$$\gamma\left(C - \hat{C}\right) = \frac{2DS_d}{r\cos\theta}\left(C - \hat{C}\right) : \text{salt dissolution source term}$$

Equation 2.2 is a mass conservation equation where the first term is the rate of salinity change; the second term is the net advective flux consisting of two parts: externally induced

volume flow (raw-water injection) and boundary layer transport. The third term is the rate of salt dissolution at the walls and the fourth term is the diffusive flux. The terms are summarized in Table 2.1.

SANSMIC:	Traditional :	Term name:	Refer to:
$\frac{\partial C}{\partial t}$	$\frac{\partial C}{\partial t}$	salinity change rate	Sect 2.1
$\left(\frac{M_0}{A} - \frac{2D}{r}\frac{\partial r}{\partial z}\right)\frac{\partial C}{\partial z}$	$u\frac{\partial C}{\partial z}$	net advective flux	Sect 2.4
$\frac{2DS_d}{r\cos\theta}\left(C - \hat{C}\right)$	$\gamma(C - \hat{C})$	salt dissolution rate	Sect 2.3
$D\frac{\partial^2 C}{\partial z^2}$	$D\frac{\partial^2 C}{\partial z^2}$	diffusive flux	Sect 2.2

Table 2.1: The mass conservation equation as used in SANSMIC with the corresponding term names and description locations.

2.1 Implicit Finite Difference Equation

In the following discussion, superscript n is the time step index and subscript i is the spatial index. A constant time step (Δt), constant vertical zone size (Δz), and a variable circular cross-section of radius (r_i) are assumed. $()_i$ is short hand notation implying subscript i for all relevant terms inside the parenthesis. Subscripts *inj*, *prd*, and *plm* designate the cell containing the injection point, the production point, and the plume stagnation level respectively. The plume covers the region from z_{inj} to z_{plm}.

Note that the finite difference (FD) equations presented below are extracted from the source code (reverse engineered) and therefore may not be in a standard form. (LeVeque, 2007) gives a good discussion of FD techniques. Recall Equation 2.1:

$$\frac{\partial C}{\partial t} + \left(\frac{M_0}{A} - \frac{2D}{r}\frac{\partial r}{\partial z}\right)\frac{\partial C}{\partial z} + \frac{2DS_d}{r\cos\theta}\left(C - \hat{C}\right) = D\frac{\partial^2 C}{\partial z^2}$$

which is presented below as an implicit finite difference:

First term (rate of change):

$$\frac{\partial C}{\partial t} = \frac{C_i^n - C_i^{n-1}}{\Delta t} \tag{2.3}$$

Second term (advective flux with upwind differencing):

$$u\frac{\partial C}{\partial z} = u_i^n\left(w_u\frac{(C_i^n - C_{i-1}^n)}{2\Delta z} + w_d\frac{(C_{i+1}^n - C_i^n)}{2\Delta z}\right) \tag{2.4}$$

where $u_i^n = \left(\frac{2D}{r}\frac{\partial r}{\partial z} - \frac{M_0}{A}\right)_i$ and in order to maintain stability:

$$\begin{cases} w_u = 0;\ w_d = 2 & \text{if } u_i > 0 \text{ (downward)} \\ w_u = 2;\ w_d = 0 & \text{if } u_i < 0 \text{ (upward)} \end{cases}$$

Note that u_i in the FD equation is the negative of the u in the mass balance equation (Equation 2.1). The advective term is discussed further in Section 2.4

Third term (source term):

$$\gamma_i^n(C - \hat{C}) = \left(\frac{2DS_d(C - \hat{C})}{r\cos\theta}\right)_i^n = \left(\frac{2\pi rDS_d(C - \hat{C})}{A\cos\theta}\right)_i^n \tag{2.5}$$

In SANSMIC, the source term uses circumference divided by area ($2\pi r/\pi r^2$) rather than its simplified form ($\frac{2}{r}$). The source term is discussed in more detail in Section 2.3.

Fourth term (diffusive flux):

$$D\frac{\partial^2 C}{\partial z^2} = \left(D_i^n\frac{(C_{i+1}^n - C_i^n)}{\Delta z} - D_{i-1}^n\left(\frac{A_{i-1}^n}{A_i^n}\right)\frac{(C_i^n - C_{i-1}^n)}{\Delta z}\right)\frac{1}{\Delta z} \tag{2.6}$$

The cross-sectional area (A) is the annulus between the outer casing and the cavern wall i.e. $A = \pi(r^2 - r_{co}^2)$. The diffusive term is discussed in more detail in Section 2.2

2.1.1 Combine Terms

Substituting Equations 2.3-2.6 into 2.1 gives the final form of the finite difference representation of Equation 2.1:

$$\begin{aligned}\frac{C_i^n - C_i^{n-1}}{\Delta t} =& \frac{u_i^n\big(w_u(C_i^n - C_{i-1}^n) + w_d(C_{i+1}^n - C_i^n)\big)}{2\Delta z} - \gamma_i^n(C_i^n - \hat{C}) \\ &+ \left(D_i^n\frac{(C_{i+1}^n - C_i^n)}{\Delta z^2} - D_{i-1}^n\frac{A_{i-1}^n}{A_i^n}\frac{(C_i^n - C_{i-1}^n)}{\Delta z^2}\right)\end{aligned} \tag{2.7}$$

Grouping like terms, the FD equation (Equation 2.7) can be written in the form:

$$\overline{A_i}C_{i-1}^n + \overline{B_i}C_i^n + \overline{C_i}C_{i+1}^n = \overline{D_i} \tag{2.8}$$

where

$$\overline{A_i} = D_{i-1}^n \left(\frac{A_{i-1}^n}{A_i^n}\right) \frac{1}{\Delta z^2} - w_u u_i^n \frac{1}{2\Delta z}$$
$$\overline{B_i} = -\left(\gamma_i^n + \frac{1}{\Delta t}\right) + (w_u - w_d) u_i^n \frac{1}{2\Delta z} - \left(D_i^n + \left(\frac{A_{i-1}^n}{A_i^n}\right) D_{i-1}^n\right) \frac{1}{\Delta z^2}$$
$$\overline{C_i} = D_i^n \frac{1}{\Delta z^2} + w_d u_i^n \frac{1}{2\Delta z}$$
$$\overline{D_i} = -\frac{C_i^{n-1}}{\Delta t} - \gamma_i^n \hat{C}$$

Equation 2.7 and Equation 2.8 are an algebraic representation of a set of M equations with M unknowns (C_i, i=1, 2, …, M) or a linear matrix equation where the (MxM) coefficient matrix is tridiagonal. (Strang, 2005) is a good linear algebra reference. The following is a tridiagonal matrix equation example.

$$\begin{bmatrix} b_1 & c_1 & 0 & \dots & 0 \\ a_2 & b_2 & c_2 & & \vdots \\ 0 & a_3 & b_3 & \ddots & 0 \\ \vdots & & \ddots & \ddots & c_{m-1} \\ 0 & \dots & 0 & a_m & b_m \end{bmatrix} \begin{bmatrix} x_1 \\ x_2 \\ x_3 \\ \vdots \\ x_m \end{bmatrix} = \begin{bmatrix} d_1 \\ d_2 \\ d_3 \\ \vdots \\ d_m \end{bmatrix}$$

The x's being solved for this particular case are the C_i's (specific gravity) where a_2, a_3, a_4,…, a_m are $\overline{A}$; b_1, b_2, b_3,…, b_m are $\overline{B}$; c_1, c_2, c_3,…, c_{m-1} are $\overline{C}$; d_1, d_2, d_3,…, d_m are $\overline{D}$; and the top and bottom boundary conditions (BCs) are moved to the right hand side (RHS) of the equation. A standard tridiagonal solver is used to solve for the x vector [x_1, x_2, x_3,…, x_m] in Appendix A and trigad.for in SANSMIC.

2.2 Diffusion

The diffusion coefficient (D) used in SANSMIC varies from a molecular diffusion value of D_{mol}=5.03e-5 ft^2/hr to an eddy diffusion value that can be several orders of magnitude larger. Eddy diffusion coefficients are used when the brine gradient is unstable (when specific gravity decreases with depth). The reader is referred to Russo's original documentation (Russo, 1981, 1983) for detailed discussions (see Equations 11-17 from (Russo, 1981) and Equation 5 and 8 from (Russo, 1983) and references (Knapp and Podio, 1979; Morton et al., 1956; Plesset and Whipple, 1974; Turner, 1973)) on the development of the effective diffusion coefficient and A1Main.for at ≈ line 935 and 1000.

$$D = D_{mol} + D_0 \left(\frac{dC}{dz}\right)_+^{1/2} (\text{Min}\{r, l\})^2$$

where:

$D_{mol} = 5.03\text{E}{-5}$ ft^2/hr (diffCoefD_Mol in the code)

$D_0 = 1.142\text{E}5$ ft$^{1/2}$/hr (diffD_0 in the code; see (Knapp and Podio, 1979))

$l = (\frac{6\pi}{\alpha})^{3/4}\Big(\frac{2\nu^2 C}{g\frac{dC}{dz}}\Big)^{1/4} \approx \beta(\frac{dC}{dz})^{-1/4}$ (see (Plesset and Whipple, 1974))

$\alpha = 0.064$ (from SPR data, with similar values given by (Hill, 1972; Morton et al., 1956))

$\beta = 0.147$ (diffBeta in the code)

$\nu =$ local kinematic viscosity ($1.7\text{E}{-5}$ ft^2/hr assumed)

β=0.147 is hardwired in the code which implies a kinematic viscosity of $1.7\text{E}{-5}$ ft^2/s for fresh water (C=1) or 1.6E−5 for "saturated" brine (C=1.2). In this document, $(\ )_+$ means that the term is used only if it is positive, otherwise it is 0. Note that if $l < r$, the gradient terms cancel. SANSMIC further modifies and enhances the diffusion near the production depth such that D is multiplied by 1.5 in the region where $i = i_{prd}$ and $i = i_{prd+1}$.

2.3 Source Term

The salt dissolution (source term) coefficient γ_i^n requires evaluation of S_d. From Equation 2.5 in which the subscript i and superscript n are now implied:

$$\gamma(C - \hat{C}) = \frac{2\pi r D S_d (C - \hat{C})}{A\cos\theta} = \frac{C_{sd} - C}{\Delta t}$$

Where the right hand side (RHS) is the rate of change in specific gravity due to the dissolution of salt in the volume increment i. Solving for S_d yields:

$$S_d = \frac{(C_{sd} - C)A\cos\theta}{2\pi r D \Delta t (C - \hat{C})}\text{: wall boundary source coefficient (see A1Main.for} \approx \text{line 1030)}$$

where:

$C_{sd} = f_{sg}(w)$: specific gravity due to dissolution of the salt walls

$w = \dfrac{CV f_{wt}(C) + C_s V_{sr}}{CV + C_s V_{sr}}$: weight percent of salt in the fluid due to dissolution

$V_{sr} = 2\pi r dz \dfrac{dr}{dt}\Delta t = 2\pi r \Delta z \Delta t (r_i^n - r_i^{n-1})$: volume of salt removed

V_{sr} is volRemove within the code and w is w within the code. $\frac{dr}{dt}$ is the salt wall recession rate (see Chapter 4), C_s is the specific gravity of rock salt (C_s=2.16), the function $f_{sg}(w)$ converts weight percent to specific gravity and $f_{wt}(C)$ converts specific gravity to weight percent. See A1Main.for at ≈ line 965 for C_{sd}, w, and V_{sr}. See Equations 6 and 5 in (Russo, 1981) for further description of w and V_{sr} respectively. Note that all masses (CV terms) are normalized by the density of water.

The functions $f_{sg}(w)$ and $f_{wt}(C)$ are defined as follows in fsg.for and fwt.for respectively:

$$f_{sg}(x) = \begin{cases} 1 + 0.726w & \text{if } w < 0.1 \\ 1.2019 & \text{if } w > 0.2632 \\ c_1 + c_2 w + c_3 w^2 & 0.1 \leq w \leq 0.2632 \end{cases}$$

where $w = x(1 + 0.000363(T - 75))^{-1}$

$$f_{wt}(C) = \begin{cases} 0.726^{-1}(C - 1) & \text{if } s < 1.0726 \\ 0.2632 & \text{if } s \geq 1.2019 \\ \frac{1}{2c_3}(\sqrt{c_2^2 + 4c_3(C - c_1)} - c_2) & 1.0726 \leq s < 1.2019 \end{cases}$$

with w=$f_{wt}(C)(1 + 0.000353(T - 75))$; adjusted to $75°F$ and where:
c_1=1.00197956678, c_2=0.67459890538, c_3=0.32350531044

The temperature dependence of both the weight percent and the specific gravity is shown in Figure 2.1. Here we see that as the temperature increases, the weight percent rises quickly while the specific gravity falls at a fairly constant rate. Note that temperature is currently fixed at 75°F

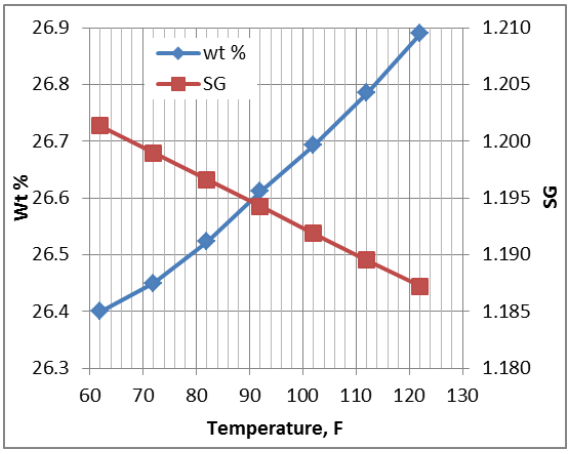

Figure 2.1: Temperature dependence of specific gravity and weight percent.

The definition of the wall angle (θ) is illustrated in Figure 2.2 where a central difference technique is used to calculate the "average" slope of the wall at depth z_i as follows:

$$\frac{dr}{dz} = \frac{r_{i+1} - r_{i-1}}{2\Delta r}$$
$$\theta = \tan^{-1}(\frac{dr}{dz})$$

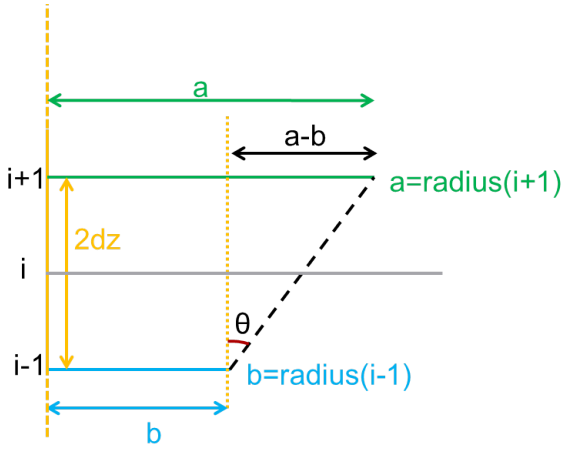

Figure 2.2: Definition of wall angle θ.

2.4 Externally Induced Flow

The externally induced flow term (M_0) in Equation 2.1 is applied over different regions of the cavern domain depending on the locations of the brine/raw water injection (z_{inj}), brine production (z_{prd}), and plume stagnation level (z_{plm}).

The flow induced by injected raw water is only applied between the plume stagnation level and the production level. That is, the plume model implicitly handles the flow from the injection point to the plume stagnation level $[z_{plm}, z_{inj}]$. In the numerical model, M_0 in Equation 2.1 is set to the user specified raw water injection rate (Q), for all cells between the plume stagnation level and the brine production level with sign determined by their relative location. Flow is from the stagnation level to the production level such that up is positive and down is negative.

2.5 Top and Bottom Boundary Conditions

The top of the grid (where $i = M$) uses a no flow, or zero gradient, boundary condition (BC). Recall Equation 2.8:

$$\overline{A_i}C_{i-1}^n + \overline{B_i}C_i^n + \overline{C_i}C_{i+1}^n = \overline{D_i}$$

such that $i+1 = M$ as it is the top boundary and let $C_M^n = C_{M-1}^n$ in order to satisfy the no flow BC then:

$$\overline{A_i}C_{M-2}^n + \overline{B_i}C_{M-1}^n + \overline{C_i}C_M^n = \overline{D_i} \Longrightarrow \overline{A_i}C_{M-2}^n + (\overline{B_i} + \overline{C_i})C_{M-1}^n = \overline{D_i}$$

At each time step the tridiagonal solver solves for $i = 1, 2, \ldots, obi - 1$. A zero local gradient is also utilized for $i = i_{obi-1}$ (the cell beneath the OBI) such that $C^n_{obi} = C^n_{obi-1}$ with $\overline{B_i} = (\overline{B_i} + \overline{C_i})$ which is the same as seen above in the zero gradient top BC. If the plume stagnation level is at $obi - 1$ then $C^n_{obi-1} = C^n_{plm}$. After solving Equation 2.7, $C^n_{obi} = C^n_{obi-1}$ for subsequent post processing.

The boundary condition at the bottom of the grid is as follows in A1Main.for at $\approx$ line 1105 (i=1 implied):

$$
\begin{aligned}
C^n &= C^{n-1} + \frac{V_{sr}\rho_s}{VC^{n-1}}\left(\frac{dC}{dw}\right) + \Delta C_D + \Delta C_{snk} \\
V_{sr} &= \pi r\left(\frac{dr}{dt}\right)\Delta t \Delta z \\
\Delta C_D &= \frac{D_e \Delta t (C_2^{n-1} - C_1^{n-1})_+}{\Delta z^2}
\end{aligned}
$$

$$
\Delta C_{snk} = \frac{Q\Delta t(C_{inj} - C^n)}{VC^{n-1}}\left\{\frac{w_1 C_1^{n-1} - w_2 C_2^{n-1}}{C_1^{n-1} - 1}\right\}\frac{dC}{dw} \text{ ; if } i_{prd}{=}1 \tag{2.9}
$$

$$
\begin{aligned}
D_e &= D_0\beta^2 \\
\frac{dC}{dw} &= 0.726 \\
w &= f_{wt}(C^{n-1})
\end{aligned}
$$

The above has been reverse engineered from the source code, but the authors have not reconciled the theoretical and implemented purpose of the above. Note that V_1 (the bottom cavern cell) is adjusted to account for loss of volume as a result of insolubles. The change in specific gravity at the boundary is a function of the flow in from cell 2 by advection and diffusion, salt dissolution and possibly flow out through the production string. As before $(\ )_+$ means to use the value only if it is positive otherwise it is set to 0, that is, the term is only used when gradient is unstable. Note that Equation 2.9 is implemented differently in SANSMIC than shown: the C_n term in the RHS of ΔC_{snk} must be moved to the LHS. Equation 2.9 is left in the form shown for clarity.

If the production level is located in cell 1 ($i_{prd} = 1$) then the sink term, S_{snk}, is non-zero and accounts for the loss of brine at the new saturation level at a flow rate equal to injection rate. If the injection level is in cell 1 ($i_{inj} = 1$) then $C_1^{n-1} = C^n_{inj} = C^n_{plm}$ as described above in Section 2.5. If, for some odd reason, the plume stagnation level is in cell 1 then $C^n_1 = C^n_{plm}$.

The mass balance equation presented here is not completely understood at this time, particularly the C_{inj} and $\{\ \}$ terms in ΔC_{snk}. This should be investigated further. Experience has shown that the specific gravity below the plume is typically the value of saturated brine or increases to near saturated brine.

2.6 Coupling with the Plume

Solving Equation 2.8 for C_i^n gives:

$$C_i^n = \frac{\overline{D_i} - \overline{A_i} C_{i-1}^n - \overline{C_i} C_{i+1}^n}{\overline{B_i}}$$

Which provides a method for forcing the specific gravity (C_i^n) at any location. Letting $\overline{D_i} = 1\text{E}20 C_{plm}$ and $\overline{B_i} = 1\text{E}20$ gives:

$$C_i^n = \frac{1\text{E}20 C_{plm} - \overline{A_i} C_{i-1}^n - \overline{C_i} C_{i+1}^n}{1\text{E}20} \approx \frac{1\text{E}20 C_{plm}}{1\text{E}20} = C_{plm}$$

It is important to note that SANSMIC forces the specific gravity for all cells in the plume from the injection level to the plume stagnation level to C_{plm} using this method. C_{plm} is determined by a mass balance between the injected raw water, dissolved salt and diffused salt in a control volume consisting of the region between the injection and stagnation levels. The mass balance equation is as follows in A1Main.for at ≈ line 935:

$$C_{plm} = \overline{C} + \left(\frac{Q \Delta t (C_{inj} - \overline{C})}{\sum V_i C_i} + \frac{\sum M_i^{sr}}{\sum V_i C_i} + \frac{V_{plm} D_{plm} \Delta t (C_{plm}^0 - C_{plm})}{\Delta z^2 \sum V_i C_i} \right) \left(\frac{dC}{dw} \right) \qquad (2.10)$$

with

$$\overline{C} = \frac{\sum V_i C_i}{\sum V_i} \quad : \text{average specific gravity in the plume (C\_bar in code)}$$

$$M_i^{sr} = 2\pi r_i \frac{dr_i}{dt} \Delta z \Delta t \rho_s \quad : \text{salt mass dissolved in cell } i \text{ (totBrineWeight in code)}$$

$$V_{plm} = \Sigma \pi r_{plm}^2 \Delta z : \text{volume in the plume (totVolPlume in code)}$$

Summations are over the cells between the injection point and the plume stagnation level. The terms inside brackets in Equation 2.10 are weight percentage contributions from the net flux, sources due to wall recession, and diffusion into the top cell of the plume only. C_{inj} is the specific gravity of the injected raw water. $\frac{dC}{dw}$ is the change in specific gravity per change in weight percent, assumed to be 0.726. $\sum V_i C_i$ is the total salt mass in the plume normalized by the specific gravity of water.

Equation 2.10 reflects the changes made to the plume model between 1981 and 1983. The 1981 version performed the mass balance only for the cell containing the plume stagnation level which became an internal boundary condition for Equation 2.1 dividing the cavity domain into two regions: one above the stagnation level the other below the stagnation level. Thus, the specific gravity of the cells within the plume region was determined by the mass balance equation (Equation 2.1). Russo's documentation, (Russo, 1983) notes the change but does not provide the new equations. Note also that Equation 2.10 is implemented differently than shown in SANSMIC, the C_{plm} term in the RHS must be moved to the LHS. Equation 2.10 is left in the form shown for clarity.

2.7 Implications of Plume Model and Mass Balance Coupling

The combination of no externally induced flow and constant SG within the plume region implies that the advective terms in the mass balance equation (Equation 2.1) are zero and the SG gradient is zero (zero diffusion). That leaves only the source term, which taken in isolation, generates a uniform wall recession rate. However, the recession rates are modified by a combination of several adjustment factors (see Chapter 4) that result in wall recession rates that vary with height. This implies that much of the cavern shape within the plume region is defined by the recession-rate adjustment factors, which if tied to input, could be used as tuning parameters. The percentage of the cavern height covered by the plume region varies significantly from small for typically tall slender SPR caverns to large for short squat remedial leach configurations and bench scale simulations. Thus, plume coverage could be a significant contributor to the relative accuracy of SANSMIC under different model configurations. Recall that the injection rate and cavern radius are also contributors to plume height.

2.8 Raw Water Injection Jet Model

A previously undocumented simple injection jet model estimates the jet length as the distance traveled by the injected water in half a second, where the injection velocity is calculated as the volumetric injection rate divided by the cross-sectional area of the inner brine string as follows:

$$l_{jet} = 0.5\frac{Q}{3600\pi r_{pi}^2} \text{ : see A1Main.for} \approx \text{line 490 and line 715}$$

Where Q is the injection rate in ft^3/hr, and r_{pi} is the inner pipe radius in ft. The user provided injection location ($\overline{Z}_{inj}$) is lowered by the length of the jet (l_{jet}): $z_{inj} = \overline{Z}_{inj} - l_{jet}$. z_{inj} and is the injection point for the plume model. The plume-model injection-point radius (b_0) and injection point velocity (u_0) are also defined by the jet parameters:

$$b_0 = \text{Max}\{l_{jet}, 2r_{co}\} \text{ ; plume model injection point radius (RO in code)}$$
$$u_o = \frac{Q}{3600\pi b_0^2} \text{ ; injection point velocity (UO in code)}$$

Where r_{co} is the outer radius of the outer casing. Note that the plume velocity is in ft/s, which is inconsistent with the time units (hours) used in the rest of the code. This does not create any problems because plume velocities are only used within the plume model.

There are four string parameters specified in the SANSMIC input file: RPI, the inside radius of the inner tubing is used to calculate the jet length, RPO, the outer radius of the inner pipe is not used; RCASI, the inside radius of the outer casing is not used; and RCASO, the

outer radius of the outer casing is used to calculate the plume initial radius and to establish an annulus for vertical flow within the cavern. For further detail concerning the input file variables see Appendix B.

2.9 Mixing Due to Unstable Gradient

The following, previously undocumented, logic is applied once across the whole grid at the end of the time step. The logic amounts to swapping the smaller volume of adjacent cells that are unstable, working up from the bottom of the grid (see A1Main.for $\approx$ line 1155).

$$
\begin{aligned}
&\text{If } r_{i+1} < r_i : \\
&\qquad C_{i+1} = C_i \\
&\qquad C_i = F_{sg}\Big(\frac{\Delta VC_i w_i + M_{i+1} w_{i+1}}{\Delta VC_i + M_{i+1}}\Big) \\
&\text{If } r_{i+1} > r_i : \\
&\qquad C_i = C_{i+1} \\
&\qquad C_{i+1} = F_{sg}\Big(\frac{\Delta VC_{i+1} w_{i+1} + M_i w_i}{\Delta VC_{i+1} + M_i}\Big)
\end{aligned}
$$

Where ΔV is the volume difference between adjacent cells i and $i+1$, and $M = VC$ is the mass of brine normalized by the specific gravity.

2.10 Oil Withdrawal and Leach-Fill Logic

SANSMIC has multiple leach mode capabilities dependent upon the string locations as well as the type of injection. SANSMIC can model three types of injection: 1.) raw water is injected and oil is removed - called withdrawal leach, 2.) raw water is injected and partially or fully saturated brine is produced (or removed) - called ordinary leach in SANSMIC, and 3.) raw water is injected, oil is injected (in the case of the SPR, this is done through the oil annulus) moving the OBI down within the cavern, and partially or fully saturated brine is produced - called leach-fill. The relative string locations for the injection and production depths (when considering ordinary and leach-fill) determine whether the leach is direct or reverse leach (see Figure 1.4 and Chapter 1). Recall that direct leach occurs when z_{inj} is deeper within the cavern than z_{prd} ($z_{prd} > z_{inj}$), and reverse leach occurs when z_{prd} is deeper in the cavern than z_{inj} ($z_{inj} > z_{prd}$).

When considering the first type, withdrawal leach, the raw water displaces the oil. That is, the OBI is moved upward in increments such that displaced volume is approximately equal to injected volume. SANSMIC handles this by removing oil through the production string as in a "direct" leach in which the production depth is set to the OBI depth. In this

case, externally induced flow occurs between the plume stagnation level and the OBI.

SANSMIC also contains time step control logic that keeps the OBI from moving more than one cell in a single step.

The leach fill logic works similar to the oil withdrawal case except the OBI is moved downward in increments corresponding to the oil fill rate (Q_{fill}) and the externally induced flow between the production point and the OBI is adjusted by the oil fill rate ($M_0 = Q - Q_{fill}$).

2.11 Oil and Raw Water Injection Modification

Prior to 2014, the injection rates for oil and under-saturated brine were constant over a leach stage. In 2014, SNL developed coding logic that allowed for a table of injection rates to be read for a leach stage (near line $\approx$ 710 of A1Main.for) which provides much more flexibility. The code can currently accept a constant injection rate for the under-saturated brine and oil or look up in a table the corresponding injection rate for the current timestep, see GetQ.for. The change and increased flexibility does not change the physics or flow of the code.

2.12 Insolubles

The insolubles that are released during leaching either settle to the floor causing floor rise or are vented with the partially saturated brine. SANSMIC tracks the level of floor rise and does not continue leaching below the floor level. If the injection or production level is beneath the floor, they too are moved up to the first viable cell. The fraction of insolubles that fall to the floor as opposed to being vented is calculated in equation 7 of (Russo, 1983) at $\approx$ line 1060 of A1Main.for and shown below:

$$f = \frac{0.5}{1 + 0.00231v} + 0.5\mathrm{e}^{-0.002v} \text{ (fraction of falling insolubles; FALLF in code)}$$
$$v = \frac{\pm Q}{A} \text{ (upward fluid velocity)}$$

where Q is positive when the production cell is above the jet cell, negative when the production cell is below the jet cell, and zero when outside the region between the jet and production depth. $v = 0$ when outside the production-jet depth cell range and therefore $f = 1$. For a typical SPR cavern leach (100 ft radius, 100,000 bbls/day (BPD)) when inside the production-jet cell range, $v \approx 0.745$ and therefore $f \approx 0.9984$. For f to decrease to 0.95, the maximum flow rate of 120,000 would need to be utilized in a 40 ft radius cavern. The volume of the falling and vented insolubles is computed over each cavern cell as follows:

$$Insol_{Fall} = V_{sr} * \text{ insol ratio } * f$$
$$Insol_{Vent} = V_{sr} * \text{ insol ratio } * (1 - f)$$

Recall that V_{sr} is the volume of salt removed from Section 2.3, the insoluble ratio is given by user input.

2.13 Coalescing Caverns

As SANSMIC was originally designed for developing a cavern from one or more boreholes, the code allows the user to specify the number of boreholes to coalesce (up to 3). The code then coalesces two or three identical caverns given in the user input (see A1Main $\approx$ line 630). Assuming r_i is the given cavern radius for cell i, R is the distance given between the initial boreholes, and $r_{max} = \text{Min}\{0.5R, r_i\}$.

When coalescing 2 caverns:

$$\frac{1}{\pi}Area = r_i^2 + \frac{2}{\pi}\left(r_{max}\sqrt{r_i^2 - r_{max}^2} + r_i^2 \arcsin\left(\frac{r_{max}}{r_i}\right)\right)$$

When coalescing 3 caverns:

$$\frac{1}{\pi}Area = 1.65399(r_i - .57735R)^2 + 1.90986\left(r_{max}\sqrt{r_i^2 - r_{max}^2} + r_i^2 \arcsin\left(\frac{r_{max}}{r_i}\right)\right)$$

With the new $r_i = \sqrt{\frac{1}{\pi}Area}$.

2.14 Work Over Period

When the stage is complete, if the user has specified a delay time (or work-over time), the end time is modified by adding the delay time to the end time. The injection volume, injection rate, and oil fill volume are set to 0 before beginning the next timestep that allows the leaching of the cavern to continue.

This page intentionally left blank.

Chapter 3

Unconstrained Steady Plume Model

The undersaturated brine that is injected within the cavern is less dense than the cavern brine and thus will form an upward moving plume due to buoyant forces. The mixing within the plume is assumed to be rapid which makes an analysis of the plume dynamics considering a uniform specific gravity and velocity within the plume appropriate. Equation 6 from (Morton et al., 1956) presents a set of equations that describe the dynamics of an unconstrained steady buoyant plume as follows (see Figure 3.1 for schematic of Morton's plume model configuration):

$$\begin{aligned} \frac{d(b^2u)}{dz} &= 2\alpha bu \quad : \text{volume balance} \\ \frac{d(b^2u^2)}{dz} &= 2b^2g(C_o - C) \quad : \text{momentum balance} \\ \frac{d(b^2ug(C_o - C))}{dz} &= 2b^2ug\frac{dC_o}{dz} \quad : \text{density deficiency (equivalent to heat)} \end{aligned} \tag{3.1}$$

where

$b =$ effective plume radius (ft)
$C =$ brine specific gravities in the plume
$C_o =$ brine specific gravities out of the plume
$u =$ plume velocity in vertical (z) direction (ft/s)
$g =$ acceleration due to gravity (32.174 ft/s^2) (G in the code)
$\alpha =$ entrainment coefficient (set to 0.09) (ALPHA in the code)

Equations 3.1 are three equations with three unknowns (b, C, u). Injection point boundary conditions (b_0, u_0) are provided by the injection jet model (Section 2.8); $C(t) = C_{inj}$ and C_o is the solution to Equation 2.1 from the previous time step. Only the elevation of the top of the plume (stagnation level) is used by SANSMIC. Every third time step, Equations 3.1 are solved using the Sandia library routine ODE which integrates a system of N first order ODEs of the form: $y_i' = \frac{dy_i}{dz} = F(z, y_1, y_2, \ldots, y_n)$ given $y_i(z)$ and a subroutine to evaluate y_i' set up in plume.for and the ODE is solved using ode.for, de.for, and step1.for. For solution

of Equation 3.1, let:

$$y_1 = b^2 u \qquad y_1' = 2\alpha\sqrt{y_2} \qquad u = \frac{y_2}{y_1} \tag{3.2}$$

$$y_2 = b^2 u^2 \qquad y_2' = 2\frac{y_3}{u} \qquad b = \sqrt{\frac{y_1}{u}} \tag{3.3}$$

$$y_3 = b^2 u g(C_o - C) \qquad y_3' = 2y_1 g\frac{dC_o}{dz} \qquad C = C_o - \frac{y_3}{y_1 g} \tag{3.4}$$

Where y_1', y_2', and y_3' are seen in a slightly different form in Equation 7 of (Morton et al., 1956). Equations 3.2-3.4 are integrated as a function of z_i from the injection point z_{inj} upward until one of the following criteria is met:

$$u_i < 1\text{E}{-6},$$
$$b_i > 0.7 r_i \text{ or}$$
$$z_i > z_{obi}$$

This elevation is called the plume stagnation level (z_{plm}). It is the level at which the plume has risen and grown until it interacts with the cavern wall (plume radius is 0.7 that of the cavern radius).

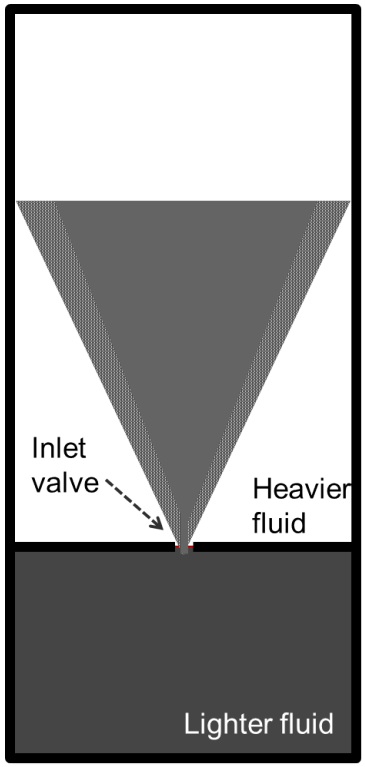

Figure 3.1: Schematic of plume experiments from (Morton et al., 1956).

Chapter 4

Salt Wall Recession Rate Model

The recession rate of a large vertical wall of salt dissolving under the influence of natural convection can be correlated as a function of only the bulk fluid specific gravity at T= 75°F in ft/s as follows:

$$\frac{dr}{dt} = a_1 C^4 + a_2 C^3 + a_3 C^2 + a_4 C + a_5 + a_6 C^{-1}\text{: see fpa.for for evaluation} \tag{4.1}$$

$$\begin{aligned} a_1 &= 0.76091661297 & a_2 &= -3.8715516531 & a_3 &= 7.8254117638 \\ a_4 &= -7.8395924067 & a_5 &= 3.8789476581 & a_6 &= -0.7533873462 \end{aligned}$$

Equation 4.1 is the same as Equation 3 from (Russo, 1981) and Equation 1 from (Russo, 1983) except that the coefficients in Equation 4.1 are divided by 60 as $\frac{dr}{dt}$ is calculated in ft/s (see fpa.for in the code) then converted to ft/hr by multiplying by 60.

The recession rate varies with wall angle (θ) measured from vertical such that $\theta = 0°$ is an upward facing surface shown in Figure 4.1 where θ is the angle from vertical to the salt wall position. Recall that the angle θ is calculated in Section 2.3 and specifically shown in Figure 2.2. The interpretation of θ in a cavern setting is seen in Figure 4.2

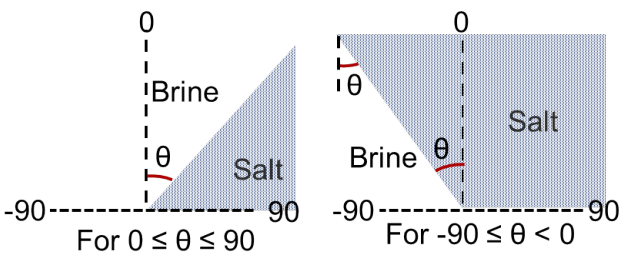

Figure 4.1: Wall angle definition.

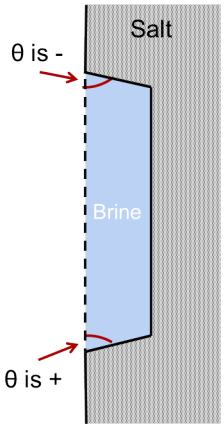

Figure 4.2: Wall angle definition in the cavern setting.

Equation 4 from (Russo, 1981) and Equation 2 from (Russo, 1983) is $\frac{dr}{dt}\Big|_{\theta>0 \text{ or } \theta<0} = \frac{dr}{dt}\Big|_{\theta=0} *$ (incline factor) where the incline factor is the following from (Saberian and Podio, 1977):

$$\left.\frac{dr}{dt}\right|_{\theta>0} = \left.\frac{dr}{dt}\right|_{\theta=0} * f_{\theta+} = \left.\frac{dr}{dt}\right|_{\theta=0} * (\cos\theta)^{1/2}$$

$$\left.\frac{dr}{dt}\right|_{\theta<0} = \left.\frac{dr}{dt}\right|_{\theta=0} * f_{\theta-} = \left.\frac{dr}{dt}\right|_{\theta=0} * \left(1 + 0.22\left(1 \pm \left|\frac{\theta + 45^\circ}{45^\circ}\right|^{1/3}\right)\right)$$

However, the implementation is slightly different. The code distinguishes between the two cases by checking $\tan(\theta)$ instead of θ.

The $\pm$ given in the second case ($f_{\theta-}$) is dependent upon whether θ is greater or less than -45. When $\theta < -45$, $+$ is used. When $\theta > -45$, $-$ is used instead. The incline factor as computed in the code is shown in Figure 4.3 for the possible range of θ, [-90,90].

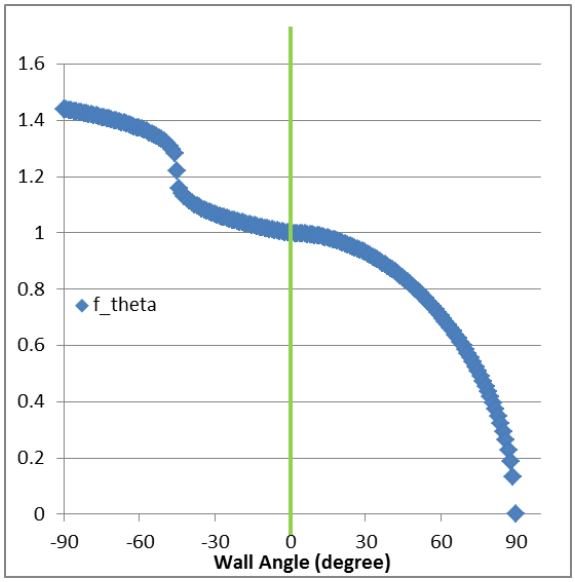

Figure 4.3: Incline factor for $-90 < \theta < 90$.

The SANSMIC final recession rate is as follows in A1Main.for at ≈ line 925:

For direct leach:

$$\frac{dr}{dt} = (f_d \text{ or } f_T)(f_{ins} \text{ and } f_v) f_\theta \left.\frac{dr}{dt}\right|_{\theta=0}$$

For reverse leach:

$$\frac{dr}{dt} = \big((f_d \text{ or } f_T) + f_{RL}\big) f_\theta \left.\frac{dr}{dt}\right|_{\theta=0}$$

where:

f_θ - adjustment factor for wall angle as discussed above (always used)

f_d - default adjustment factor which can be used to adjust the basic recession rate equation if site specific data are available. A constant value can be input or it can be specified as a function of height within the code. (usually 1.0)

f_T - temperature adjustment factor (overrides f_d, see Section 4.1)

f_{RL} - adjustment term for reverse leach (applied from i_{inj} to i_{obi}, see Section 4.4)

f_{ins} - adjustment factor for direct leach due to insolubles (applied from i_{inj} to i_{plm}, see Section 4.2)

f_v - velocity adjustment factor for direct leach (applied from i_{plm} to i_{prd}, $i_{prd} > i_{plm}$, see Section 4.3)

The temperature adjustment has not been used (temperature has always been 75°F) and the default factor f_d has always been 1.0.

4.1 Temperature Correction

Temperature is hardwired to 75°F. However there is temperature adjustment logic in the code at ≈ line 670 of A1Main.for:

$$f_T = \Big(\frac{T + 460}{535}\Big)^{0.75} e^{0.01(T-75)}$$

which is applied to all cells if the default factor $f_d > 0.92$. The factor as a function of temperature is shown in Figure 4.4.

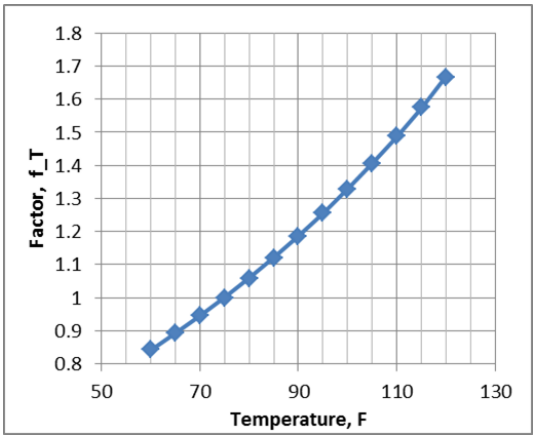

Figure 4.4: Adjustment factor f_T.

4.2 Direct Leaching Insolubles Adjustment Factor

The following dissolution rate factor is applied between the injection level and the plume stagnation level for direct leach if the default factor f_d or temperature factor $f_T > 0.9$ (see A1Main.for line ≈ 800):

$$f_{ins} = 0.9 + 0.05 \frac{r_{inj}}{\text{Max}\left\{z_{plm} - z_i, \frac{r_{inj}}{2}, 0.01\right\}}$$

The effect is to generate adjustment factors that vary roughly from 0.9 at the injection point to 1.0 at the plume stagnation level. This can be seen in Figure 4.5 assuming a typical SPR cavern height of 2000 ft, with a plume height taken to be 1000 ft, the injection depth 700 ft, and the injection radius taken to be 50 ft.

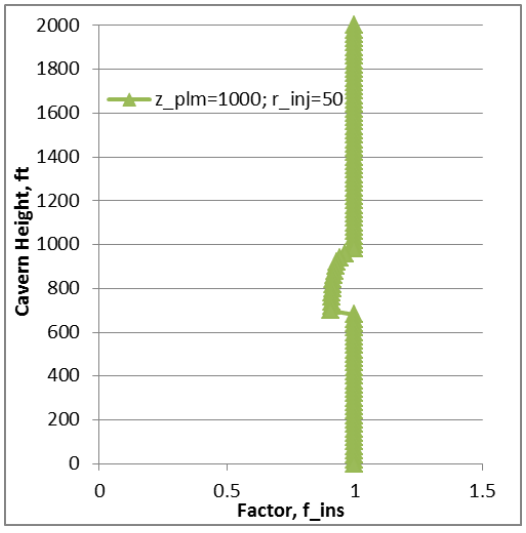

Figure 4.5: Adjustment factor f_{ins}.

4.3 Direct Leaching Velocity Adjustment Factor

If the production level is above the plume stagnation level the following correction factor is applied between those points if the bulk flow velocity ($\frac{Q_i}{\pi r^2}$) > 100 ft/hr (see A1Main.for line $\approx$ 810):

$$F_{vel} = a_1 + a_2 u_i + a_3 u_i^2 + a_4 u_i^3$$

where:

$a_1 = 0.98077$ $a_2 = -4.363\,76\text{E}{-4}$ $a_3 = 5.3574\text{E}{-7}$ $a_4 = 6.614\,53\text{E}{-11}$ and

$$u_i = \text{Min}\Big\{\frac{Q_i}{\pi r^2}, 4700\Big\}$$
$$f_v = \text{Min}\{F_{vel}, 4\}$$

The default dissolution rate factor (usually 1.0) is multiplied by f_v. Assuming a maximum injection rate of 120,000 bbls/day which is reasonable for the SPR, f_v is only calculated for radii smaller than 2.85 ft (i.e. f_v only kicks in at small cavern radii with large injection rates).

4.4 Reverse Leaching Adjustment Factor

For reverse leaching with the injection point well below the oil blanket, the dissolution rate is larger than predicted by Equation 4.1. A heuristic model based on empirical fits is used to calculate a dissolution enhancement term, f_{RL}, as follows:

Region between the injection point and the oil blanket (see A1Main.for $\approx$ line 860:)

$$f_{RL} = \frac{1}{120}\text{Min}\Big\{\frac{L\Delta z}{200}, 2, \frac{r_{inj}}{25}\Big\}\sqrt{Q_i}\Big((1-0.4L_r)L_r\Big)^{1/3} \tag{4.2}$$

Region below the injection point:

$$f_{RL} = f_{RL}|_{z_{inj}}\, e^{-2.5L_r}$$

Where

$$L_r = \frac{L_v}{L} \text{ : (DUM in the code at line 875, but changes throughout code)}$$
$$L = \frac{1.15(z_{obi} - z_{inj})}{\Delta z} \text{ : (DUML in the code)}$$
$$L_\nu = L - \frac{z_{obi} - z}{\Delta z} \text{ : (DUMV in the code)}$$

The Δ z term in L and L_ν converts distances into number of zones. f_{RL} is added to the inputted default salt dissolution factor, which is usually 1.0. Note that Equation 4.2 is

slightly different than documented in the original documentation (Russo, 1983). Assuming a normal SPR cavern height of 2000 ft, Q_i=11697.1 (100,000 bbls/day), with the injection radius being 50 ft, and the injection height being 1500 ft the corresponding adjustment factor as a function of cavern height is given in Figure 4.6.

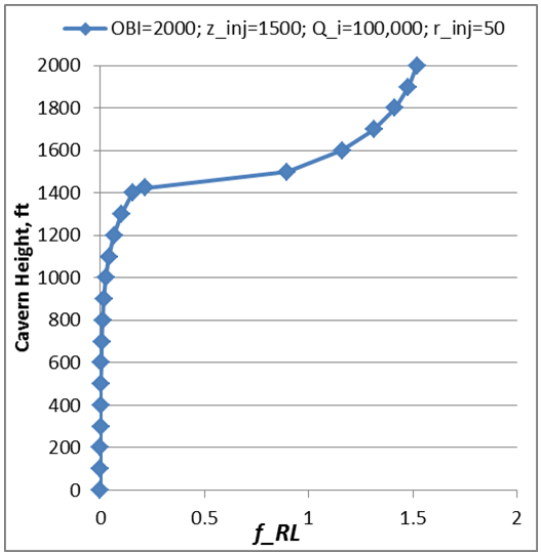

Figure 4.6: Adjustment factor f_{RL}.

The discrepancy between the original predicted dissolution rate and the observed leaching pattern is first noted in (Russo, 1983) in the section entitled "Dissolution Rate Correction". There it is theorized that:

> "the dissolution correlations are only valid when the bulk fluid flow velocities are much less than the peak boundary layer velocity. For [this] case, the plume rising near the center of the cavern and the return flow along the periphery generate a toroidal vortex, the velocity of which may be much greater than that calculated for plain plug flow. An accurate model of the vortical velocity field, which is a function of raw water injection rate, pipe string settings, and cavern geometry has not yet been included in the code."

Chapter 5

Path Forward

Recently, an increase in research has focused on understanding and developing the dissolution rate and injection plume characteristics over various parameter ranges such as undersaturated brine temperature in (Engvall et al., 2013), injection rates in (O'Hern et al., 2011), and injection depth relative to the bottom of the cavern (impinging) (Heath et al., 2015). This work has not been incorporated into the current version of SANSMIC. Temperature effects could be activated within SANSMIC by fully implementing the temperature dissolution rate factor as described in Section 4.1 and closely reviewing the code for all impacts and modifying sub-models as necessary (SG and weight percent for example). For each improvement and update to the source code, the code will then be tested against the available validation data sets as documented in (Weber et al., 2014), documented within the source code, and formally documented and held in the SPR library.

This page intentionally left blank.

Chapter 6

Conclusions

The SANSMIC design document is intended to bring more clarity and provide greater explanation to the source code. To that end: the source code and document reference each other; the program flow is outlined (see Section 1.3): details in the historical documentation are either referenced or repeated; code features that were added later or were not documented previously have been expounded. No major modifications (no change in the code's physics) have occurred since the original documentation (Russo, 1981, 1983) although recent experiments may yield improvements to the temperature, dissolution, and plume methods.

Future changes to the code will be thoroughly documented within the code itself, retained in SPR records in report form, and checked against the validation data utilized in (Weber et al., 2014).

The majority of the work presented in this document has been inferred from reverse engineering the source code and is the best representation from the authors' perspective.

The mathematical and numerical models discussed above were extracted from the SANSMIC source code, compared to those in Russo's original documentation (Russo, 1981, 1983) and are reported as implemented. A summary of the changes and additions to the original documentation are provided in Table 6.1. The models and equations form the basis of this SANSMIC as-built design document. This design document is the second of four major components of the QA and benchmarking process to be performed on SANSMIC consisting of: 1) requirements or capabilities, 2) design, 3) verification and validation (see (Weber et al., 2014)) and 4) user instructions.

Topic:	Comment:
Diffusion coefficients	Updated summary discussion and updated parameter values
Finite difference solution method for mass balance equation	New discussion of previously undocumented logic: FD equations, solution method, source term, externally induced flow, boundary conditions
Coupling of mass balance and plume models	Mathematics of new coupling logic documented
Raw water injection jet	New discussion of previously undocumented logic. Affects injection point and plume model boundary conditions.
Mixing due to unstable gradient	New discussion of previously undocumented logic
Oil withdrawal leach mode	New discussion of implementation logic
Leach-fill mode	New discussion of implementation logic
Unconstained steady plume model	New discussion of solution method.
Salt wall recession rate model	New discussion of 3 previous undocumented adjustment factors for: temperature, direct leach insolubles, direct leach high velocity flow.
Reverse leach adjustment factors	Updated discussion for reverse leach adjustment factors, new parameters in correlation equation.
Injection history table input	Added for greater input value flexibility

Table 6.1: Summary of Changes and Additions to SANSMIC Documentation.

References

L. Engvall, T.J. O'Hern, and D.L. Lord. Experimental Characterization of Temperature Dependence of Salt Dissolution Rate. Technical report, Solution Mining Research Institute, 22-23 April, 2013 2013.

T.J. Eyermann. Comparison of SANSMIC Simulation Results with Cavern Shapes on the SPR Project. Technical report, Solution Mining Research Institute, 1984.

J.E. Heath, M.B. Nemer, and D.L. Lord. On the Controls of Mixing of Injected Fresh Water Jets with Brine in Salt Caverns: Scaled Flow Visualization Experiments. Technical report, Solution Mining Research Institute, 2015.

B.J. Hill. Measurement of Local Entrainment Rate in the Initial Region of Axisymmetric Turbulent Air Jets. *Journal of Fluid Mechanics*, 51(4), 1972.

R.M. Knapp and A.L. Podio. Investigation of salt transport in vertical boreholes and brine invasion into fresh water aquifers. Technical report, ONWI 77, May 1979.

R. J. LeVeque. *Finite Difference Methods for Ordinary and Partial Differential Equations*. SIAM, Philadelphia, 1rst edition, 2007.

B. R. Morton, G. Taylor, and J. S. Turner. Turbulent Gravitational Convection from Maintained and Instantaneous Sources. *Proceedings of the Royal Society of London Series a-Mathematical and Physical Sciences*, 234(1196), 1956.

T.J. O'Hern, R.O. Cote, and S.W. Webb. Preliminary Investigations of Salt Wall Leaching Under Flow. Technical Report FY11-2.4(b4), Sandia National Laboratories, February 25, 2011 2011.

M.S. Plesset and C.G. Whipple. Viscous Effects in Rayleigh-Taylor Instability. *Physics of Fluids*, 17, 1974.

L. Rahm and G. Walin. On Thermal Convection in Stratified Fluids. *Geophysical and Astrophysical Fluid Dynamics*, 13, 1979a.

L. Rahm and G. Walin. Theory and Experiment on the Control of Stratification in Almost Enclosed Containers. *Journal of Fluid Mechanics*, 90, 1979b.

D.C. Reda and A.J. Russo. Experimental Studies of Oil Withdrawal from Salt Cavities via Fresh-Water Injection. Technical Report SAND83-0347, Sandia National Laboratories, March 1984 1983.

D.C. Reda and A.J. Russo. Experimental Studies of Salt Cavity Leaching via Fresh-Water Injection. Technical Report SAND84-0020, Sandia National Laboratories, March 1984 1984.

D.K. Rudeen and D.L. Lord. QA Plan for Software Used by Sandia to Support Vapor Pressure Project. Technical Report FY11-2.1(a5), Sandia National Laboratories, May 26, 2011 2011.

D.K. Rudeen, D.L. Lord, and S.W. Webb. Investigation of SANSMIC Capabilities for Simulating Historical Bench-Scale Dissolution Experiments. Technical report, 17-Jun-2011 2011.

A.J. Russo. A Solution Mining Code for Studying Axisymmetric Salt Cavern Formation. Technical Report SAND81-1231, Sandia National Laboratories, September 1981 1981.

A.J. Russo. A User's Manual for the Salt Solution Mining Code, SANSMIC. Technical Report SAND83-1150, Sandia National Laboratories, September 1983 1983.

A. Saberian and A.L. Podio. A computer model for describing the development of solution-mined cavities. Technical Report 1(1), IN SITU, 1977.

G. Strang. *Linear Algebra and its Applications*. Academic Press, INC, New York, 4th edition, 2005.

J.S. Turner. *Bouyance Effects in Fluids*. Cambridge Univ. Press, New York, 1973.

G. Walin. Contained Non-Homogeneous Flow under Gravity or How to Stratify a Fluid in Laboratory. *Journal of Fluid Mechanics*, 48(Aug 27), 1971.

P.D. Weber, D.K. Rudeen, and D.L. Lord. SANSMIC Validation. Unlimited Release SAND2014-16980, 2014.

Appendix A

Solving Tridiagonal Matrix Equations

A linear matrix equation with tridiagonal coefficient matrix is as follows:

$$\begin{bmatrix} b_1 & c_1 & 0 & \dots & 0 \\ a_2 & b_2 & c_2 & & \vdots \\ 0 & a_3 & b_3 & \ddots & 0 \\ \vdots & & \ddots & \ddots & c_{n-1} \\ 0 & \dots & 0 & a_n & b_n \end{bmatrix} \begin{bmatrix} x_1 \\ x_2 \\ x_3 \\ \vdots \\ x_n \end{bmatrix} = \begin{bmatrix} d_1 \\ d_2 \\ d_3 \\ \vdots \\ d_n \end{bmatrix}$$

Using Gaussian elimination to achieve an upper triangular set of equations results in the coefficients as follows (denoting the new modified coefficients with primes):

$$\begin{bmatrix} 1 & c'_1 & 0 & \dots & 0 \\ 0 & 1 & c'_2 & & \vdots \\ 0 & 0 & 1 & \ddots & 0 \\ \vdots & & \ddots & \ddots & c'_{n-1} \\ 0 & \dots & 0 & 0 & 1 \end{bmatrix} \begin{bmatrix} x_1 \\ x_2 \\ x_3 \\ \vdots \\ x_n \end{bmatrix} = \begin{bmatrix} d'_1 \\ d'_2 \\ d'_3 \\ \vdots \\ d'_n \end{bmatrix}$$

where:

$$c'_i = \begin{cases} \frac{c_1}{b_1} & i{=}1 \\ \\ \frac{c_i}{b_i - c'_{i-1} a_i} & i{=}2,3,\dots,n\text{-}1 \end{cases}$$

and

$$d'_i = \begin{cases} \frac{d_1}{b_1} & i{=}1 \\ \\ \frac{d_i - d'_{i-1} a_i}{b_i - c'_{i-1} a_i} & i{=}2,3,\dots,n \end{cases}$$

In other words:

$$\begin{bmatrix} 1 & \frac{c_1}{b_1} & 0 & \dots & 0 \\ 0 & 1 & \frac{c_2}{b_2 - c'_1 a_2} & & \vdots \\ 0 & 0 & 1 & \ddots & 0 \\ \vdots & & \ddots & \ddots & \frac{c_{n-1}}{b_{n-1} - c'_{n-2} a_{n-1}} \\ 0 & \dots & 0 & 0 & 1 \end{bmatrix} \begin{bmatrix} x_1 \\ x_2 \\ x_3 \\ \vdots \\ x_n \end{bmatrix} = \begin{bmatrix} \frac{d_1}{b_1} \\ \frac{d_2 - d'_1 a_2}{b_2 - c'_1 a_2} \\ \frac{d_3 - d'_2 a_3}{b_3 - c'_2 a_3} \\ \vdots \\ \frac{d_n - d'_{n-1} a_n}{b_n - c'_{n-1} a_n} \end{bmatrix}$$

This is termed the forward sweep. The solution is then obtained by back substitution:

$x_n = d'_n$

$x_i = d'_i - c'_i x_{i+1}$; for $i = n-1, n-2, \ldots, 1$.

This calculation is conducted in trigad.for.

Appendix B

Input and Output Files

The following is a very brief, very coarse description of the input file accepted by SANSMIC. An updated User's Manual that goes into greater detail on the input and output files' content and format is planned for FY16. The coarse initial geometry of the cavern is shown in Figure B.1. This geometry is used in the example input files shown in Table B.1 and Table B.2. The input files are identical except in the way in which the geometry data is entered. Table B.1 uses radial data (idata=0) and Table B.2 uses depth and volume data (idata=1).

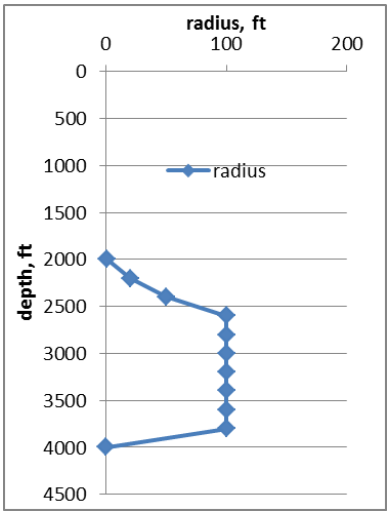

Figure B.1: Geometry of the cavern used in the example input file.

1a	**Stage 1 - DD 1**								
2a	10	1	1680	0	0	720	1	0	-0.0
3a	2000.	100.0	100.0	200.0	150.0				
4a	100000.0								
5a	4.925	5.3750	4.925	5.3750					
6a	1.0025	1.2019							
7a	.1	1800							
8a	0.0	0.0	0.0						
9	0.0								
9	100.0								
9	100.0								
9	100.0								
9	100.0								
9	100.0								
9	100.0								
9	100.0								
9	50.0								
9	20.0								
9	1.0								
10	1.0	0.04	4000.	4000.					
1b	**Stage 2 - DD 2**								
2b	10	1	1680	1	0	2160	1	0	-0.0
3b	2000.	100.0	100.0	200.0	150.0				
4b	100000.0								
5b	4.925	5.3750	4.925	5.3750					
6b	1.0025	1.2019							
7b	.1	1800							
8b	0.0	0.0	0.0						

Table B.1: Sample Input File Using Radial Data. Column 1 is line identifier and column 2 begins the actual input file.

1a	**Stage 1 - DD 1**								
2a	10	1	1680	0	0	720	1	1	-0.0
3a	2000.	100.0	100.0	200.0	150.0				
4a	100000.0								
5a	4.925	5.3750	4.925	5.3750					
6a	1.0025	1.2019							
7a	.1	1800							
8a	0.0	0.0	0.0						
9	11								
9	4000	3800	3600	3400	3200	3000	2800	2600	2400
9	2200	2000							
9	8158227	8158227							
9	7039144	5920061							
9	4800978	3681895							
9	2562812	1442729							
9	324646	44875							
9	112								
10	1.0	0.04	4000.	4000.					
1b	**Stage 2 - DD 2**								
2b	10	1	1680	1	0	2160	1	1	-0.0
3b	2000.	100.0	100.0	200.0	150.0				
4b	100000.0								
5b	4.925	5.3750	4.925	5.3750					
6b	1.0025	1.2019							
7b	.1	1800							
8b	0.0	0.0	0.0						

Table B.2: Sample Input File Using Depth vs. Volume Data. Column 1 is line identifier and column 2 begins the actual input file.

Table B.3 shows the same input file (shown in Table B.1 and Table B.2), except without the geometry data included (marked with "Cavern Data"). It now shows the input values in black, the input variable name in red, and a comment in blue. Each input file line is separated by a horizontal line and the line numbers corresponding to Table B.1 and Table B.2 are again shown on the left. The second line of the file (2a) is long and requires extended comments and details that are provided in a later table. Note that lines 9 and 10 are only specified in the first stage.

1a	Stage 1 - DD 1								
	first	comment	line						
2a	10	1	1680	0	0	720	1	0	-0.0
	ndiv	leachType	iprnt	repeat	resetGeo	iwait	nco	idata	ivol
3a	2000.	100.0	100.0	200.0	150.0				
	zmax	zi	zp	zb	zu				
	cav height	inj	prod	OBI	ullage				
4a	100000.0								
	qi								
	$InjRate_{RW}$								
5a	4.925	5.3750	4.925	5.3750					
	rpi	rpo	rcasi	rcaso					
	rad_{in}	rad_{out}	$casing_{in}$	$casing_{out}$					
6a	1.0025	1.2019							
	sgInj	sgCav							
	sg_{inj}	sg_{cav}							
7a	.1	1800							
	dt	tend							
	Δt	t_{end}							
8a	0.0	0.0	0.0						
	qfil	tdlay	sep						
	$InjRate_{Oil}$	$delay_{oil}$	$dist_{coalesce}$						
9	Cavern Data								
10	1.0	0.04	4000.	4000.					
	zdis	zfin	refdep	depth					
	dis factor	insol ratio	$depth_{ref}$	$depth_{low}$					
1b	Stage 2 - DD 2								
	second	comment	line						
2b	10	1	1680	1	0	2160	1	0	-0.0
	ndiv	leachType	iprnt	repeat	resetGeo	iwait	nco	idata	ivol
3b	2000.	100.0	100.0	200.0	150.0				
	zmax	zi	zp	zb	zu				
4b	100000.0								
	qi								
5b	4.925	5.3750	4.925	5.3750					
	rpi	rpo	rcasi	rcaso					
6b	1.0025	1.2019							
	sgInj	sgCav							
7b	.1	1800							
	dt	tend							
8b	0.	0	0						
	qfil	tdlay	sep						

Table B.3: Input File Description.

A further description of the variables is given in Table B.4 and continued in Table B.5 (ln in Tables is line number). The line number as given in Table B.3 is given, as well as the variable name, the variable type, and the description. Typical values for the SPR and general use are given in the description where relevant.

ln	Variable Name	Type	Description
2	ndiv	int	Number of nodes - 1 (maximum of 500)
2	leachType	int	Type of leach: 0=ordinary leach (direct or reverse); 1 = oil withdrawal; 2 = simultaneous leach-fill (see Sect. 2.10)
2	iprnt	int	Print every iprnt time steps. Printouts occur every iprnt*dt hours
2	repeat	int	Repeat: 0=first stage data set; 1 = subsequent stage dataset
2	resetGeo	int	Restart: 0 - no longer supported
2	iwait	int	Workover period: hrs of workover at the end of the stage
2	nco	int	Number of coalescing caverns - typically 1
2	idata	int	Type of cavern geometry: 0 = radius; 1 = depth vs. vol; -1 = depth(i), vol(i) pairs; 2 = depth(i), radius(i) pairs
2	ivol	int	Leach Volume: total vol to leach to if positive; 0 = ignored
3	zmax	real	Height of the cavern - zmax is divided into ndiv regions
3	zi	real	Height of the injection string from the cavern bottom
3	zp	real	Height of the production string from the cavern bottom
3	zb	real	Height of OBI: OBI height; 0 = use previous location OBI of previous stage
3	zu	real	Height of the ullage reference point
4	qi	real	Raw water injection rate in bbls/day - if the value is constant over each stage, a float is used here, otherwise the name of the table of fill values is read from the file
5	rpi	real	Inside radius of inner hanging string (inches)
5	rpo	real	Outside radius of inner hanging string (inches) - not used
5	rcasi	real	Inside radius of casing (inches) - not used
5	caso	real	Outside radius of casing (inches)
6	sgInj	real	Specific gravity of injected raw water
6	sgCav	real	Initial specific gravity of the in-cavern brine
7	dt	real	Computational time step
7	tend	real	End time of the stage
8	qfil	real	Oil injection rate in bbls/day - if the value is constant over each stage, a float is used here, otherwise the qi file is used
8	tdlay	real	Delay of leach due to residual oil - typically 0
8	sep	real	Distance (ft) separating the well centers when nco =2 or 3

Table B.4: Input File Variable Description.

ln	Variable Name	Type	Description
9	Cavern data (radius)	real	When idata = 0, the radius data is used starting from the bottom (see Table B.1)
9	Cavern data (depth/vol)	real	When idata = 1, the first entry is the number of data points given (ndiv+1), the depth data is then given in succession starting at the bottom and then the corresponding cumulative volume is given (see Table B.2)
9	Cavern data (dep/rad pairs)	real	When idata = -1, the first entry is the number of data points given (ndiv+1), the depth and radius pair data is then given in succession (separated by commas) starting at the bottom
9	Cavern data (depth/vol pairs)	real	When idata = 2, the first entry is the number of data points given (ndiv+1), the depth data and volume pair data is then given in succession (separated by commas) starting at the bottom
10	zdis	real	Salt dissolution factor - typically 1
10	zfin	real	Average volume ratio of insolubles to salt - typically 0.04 for SPR
10	refdep	real	Reference depth at which the plot abscissa begins - not used
10	depth	real	Depth of the cavern bottom

Table B.5: Input File Variable Description. Lines 9 and 10 are specified in the first stage only.

There are multiple output files (filenameroot.*) with extensions (ddl, dra, log, out, rad, tst) that differentiate content. All I/O files will be discussed in greater detail in the upcoming User's Manual. Broadly speaking:

- .dra file contains change in radius profiles at specified times
- .log file echoes the input file as it is read and shows read errors and runtime statistics
- .out file contains complete sets of cell data for each printed timestep
- .rad contains radius profile data at specified times
- .tst file contains a data history table at one day time increments

Appendix C

Source Code Variable Name Changes

A listing of the old variable names and new variable names are provided in Table C.1. Fortran77 did not allow for long and descriptive variable names, but the current code is used within a Fortran90 developer environment allowing the names to be expanded. The key for the new variable names is as follows:

cav cavern

coef coefficient

diff diffusion

inj injection

insol insolubles

max maximum

min minimum

obi oil-brine interface

plm plume

prod production

rad radius

sg specific gravity

tot total

vel velocity

vol volume

New Variable Name	Old Variable Name	Variable type
leachType	IDR	integer
repeat	IRPT	integer
resetGeo	IRST	integer
injCell	IZI	integer
prodCell	IZP	integer
obiCell	IZB	integer
obiCellBelow	IZBM	integer
injCellBelow	IZIM	integer
sgInj	SGI	real
sgCav	SGCF	real
numTStep	NTS	integer
diffBeta	CAF	real
diffBetaSquar	CAFS	real
diffCoefD_Mol	AKDD	real
diffCoeff	AKD	real
diffD_0	DFAC	real
tanTheta	TNAV	(real)501
cavRadius	RC	(real)501
cosTheta	CTHET	(real)501
jetPlumeCell	JPL	integer
jetPlumeCellBelow	JPLM	integer
plumeSG	CIPLM	(real)501
plumeVel	UPLM	(real)501
plumeRad	RPLM	(real)501
C_plm	CPLM	real
totBrineWeight	TMSOS	real
totVolPlume	VOLPL	real
totWeightPlume	VJPL	real
C_bar	CAV	real
volInjSigned	AMO	(real)501
recessionRate	RSR	real
volSaltRemove	VSR	(real)501
volRemove	VR	real
totMassSaltRemove	TMSS	real
minProdOrJet	JB	integer
maxProdOrJet	JT	integer
S_d	SD	real
volInsol	VINS	real
totBrineWeightNew	TMSN	real
totBrineWeightOld	TMSO	real
volInsolRemain	VLEFT	real
volInsolVent	VINSO	real
depthInsol	ZINS	real

Table C.1: Variable name change list.

DISTRIBUTION:

1 Wayne Elias (wayne.elias@hq.doe.gov) for distribution to DOE SPR Program Office, 1000 Independence Ave. SW Washington, DC 20585 (electronic copy)

1 Diane Willard (diane.willard@spr.doe.gov) for distribution to DOE and Fluor SPR Project Management Office, 900 Commerce Road East New Orlean, LA 70123 (electronic copy)

2	MS 0706	David Lord, 6912
2	MS 0750	Paula Weber, 6912
5	MS 0750	Carolyn Kirby, 6913
1	MS 0899	Technical Library, 9536 (electronic copy)

This page intentionally left blank.


Sandia National Laboratories